Design and Analysis of Various Bends in Heat Pipe

A Project Report

Submitted by

I. Joseph Prakash   -   71204402004

in partial fulfillment for the award of the degree
of

Master of Engineering
in
CAD/CAM

DEPARTMENT OF MECHANICAL ENGINEERING
KUMARAGURU COLLEGE OF TECHNOLOGY
COIMBATORE – 641 006

ANNA UNIVERSITY :: CHENNAI 600 025

APRIL – 2006

ANNA UNIVERSITY :: CHENNAI 600 025

BONAFIDE CERTIFICATE

Certified that this project report entitled **"Design and Analysis of Various Bends in Heat Pipe"** is the bonafide work of

    Mr. I. Joseph Prakash   -   Register No.   71204402004

Who carried out the project work under my supervision.

(Signature of the HOD)

Dr. T. P. MANI

HEAD OF THE DEPARTMENT
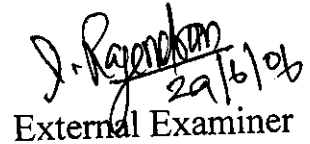
(Signature of the supervisor)

Dr. T. P. MANI

SUPERVISOR

Internal Examiner

Dr. T.P. Mani

B.E., M.E. Ph.D DML., MIE., MNIOR., MISTE.,

Dean & HoD / Dept. of Mech. Engg.

Kumaraguru College of Technology

Coimbatore - 641 006

External Examiner

DEPARTMENT OF MECHANICAL ENGINEERING

KUMARAGURU COLLEGE OF TECHNOLOGY

COIMBATORE 641 006

Optimization Techniques in Engineering Sciences and Technologies

OPTEST - 2006

held at

BANNARI AMMAN INSTITUTE OF TECHNOLOGY

Sathyamangalam-638 401 during

April 11-12, 2006

Certificate

This is to certify that Mr./~~Ms.~~/~~Mrs.~~ .....I. Joseph Prakash.....

has participated / presented a paper entitled ..... DESIGN AND ANALYSIS OF

.....VARIOUS BENDS IN HEAT PIPE.....

in the National Conference on "Optimization Techniques in Engineering Sciences and Technologies

(OPTEST-2006)" during 11-12 April 2006, organized by the Department of Mechanical Engineering,

Bannari Amman Institute of Technology, Sathyamangalam.

C SASIKUMAR/ G SASIKUMAR
Organizing Secretaries

Dr K THIRUNAVUKKARASU
Convener

Dr A SHANMUGAM
Chairman

ABSTRACT

Heat transport has been one of the most difficult and inefficient tasks in thermal management. It often results in costly heat transfer losses and reduced overall efficiencies. Performance of mechanical and electronic components inside automobiles is now governed by the efficiency of cooling system. Heat transfer by heat pipes is one of the fastest and most efficient methods for thermal management. In automobiles, the stress of modern design is on reducing bulk weight and volume of all components. The early studies mostly concentrated on heat pipes used in straight configurations. But many practical designs demand heat pipes in contorted shapes. This work investigates the feasibility of various bends in heat pipe

This work is focused on design evaluation of performance characteristics of various bends in heat pipe. The bending in heat pipes affects the capillary action, pressure drop, boiling limits and bend losses. In this heat pipe oxygen free copper is used for container and the water as the working fluid. The wick was made up of sintered cooper matting. The performance of the heat is evaluated at bend angles of $15^0, 30^0, 45^0, 60^0$ and 90^0 of the heat pipe and a mathematical model is developed for the same. The mathematical model results are validated using simulated values from "FLUENT" software. The result shows that the extent of feasibility of bendable heat pipes limits up to 90^0 in all orientations. The pressure loss and the loss in heat carrying capacity were calculated and presented.

ஆய்வு சுருக்கம்

வெப்ப மேலாண்மையில் வெப்பங்கடத்தல் என்பது ஓர் கடினமான மற்றும் பயனுறு றன் குறைந்த பணியாகும். இதன் விளைவானது அதிக வெப்ப இழப்பு மற்றும் மொத்த பனுறு திறனை குறைக்கிறது. தானியங்கு இயந்திரத்தின் உள்ளே உள்ள எந்திரவியல் ற்றும் மின்னியல் பொருட்களின் செயல்பாடானது குளிர்விக்கும் அமைப்பின் மூலம் ன்காணிக்கப்படுகிறது. வெப்ப மேலாண்மையில் வெப்ப குழாய் மூலமாக வெப்பங்கடத்தும் முறையானது வேகமான மற்றும் அதிக பயனுறுதிறன் உள்ளதாகும். தொடக்கத்தில் ஆராய்ச்சியானது நேரான வெப்பகுழாய் அமைப்பில் மேற்கொள்ளப்பட்டுள்ளது. ஆனால் பெரும்பாலான செயல்முறை செயல்பாடுகளில் வெப்பகுழாயானது பல்வேறு வடிவங்களில் தேவைப்படுகிறது.

இந்த ஆய்வின் நோக்கமானது வளைவான வெப்பகுழாயை வடிவமைத்து அதன் குணநலன்களை கணக்கிடுதல் ஆகும். வெப்பகுழாயில் உள்ள வளைவானது நுண்புழை குழாய் நிகழ்வு, அழுத்த குறைவு, கொதி நிலை அளவு மற்றும் வளைவுகளினால் ஏற்படும் இழப்பு ஆகியவற்றை பாதிக்கிறது. இந்த வெப்பகுழாயில் ஆக்ஸிஜன் இல்லாத செம்பு கொள்கலனாகவும், தண்ணீர் இயக்க நீர்மமாகவும் உபயோகிக்கப்படுகிறது. திரியானது உருக்கி இணைத்த செம்பில் உருவாக்கப்பட்டது. வெப்பகுழாயின் வெப்பத்தின் செயல்பாடானது $15°; 30° 45°, 60°$ மற்றும் $90°$ வளைவு கோணங்களுக்கு கணக்கிடப்பட்டது, மற்றும் கணிதமாதிரியானது உருவாக்கப்பட்டது. கணித மாதிரியின் விளைவுகளானது Fluent மென்பொருளின் பகிர்க்கப்பட்ட மதிப்புகளுடன் மதிப்பீடு செய்யப்பட்டன. இந்த ஆய்வின் விளைவானது $90°$ வரையுள்ள வளையக்கூடிய வெப்பகுழாயின்க் செயல்திறன் எல்லையை காட்டுகிறது. அழுத்த குறைவு மற்றும் வெப்பம் கடத்தும் தன்மையானது கணக்கிடப்பட்டுள்ளது.

ACKNOWLEDGEMENT

CONTENTS

LIST OF TABLES

LIST OF FIGURES

LIST OF SYMBOLS

M	maximum possible heat transport
ρ	density of working fluid in liquid phase
σ	surface tension of the working fluid
μ	Dynamic viscosity of working fluid in liquid phase
L	length of the heat pipe
Δpv	vapor pressure gradient
Δpl	liquid pressure gradient
$\Delta pcap, max$	capillary pressure in liquid-vapor interface
$\Delta pe, phase$	phase change taking place at the evaporator
$\Delta pc, phase$	phase change taking place at the condenser
Δpg	phase change due to gravity
r_{eff}	effective capillary radius
σ	surface tension
Re_r	radial Reynolds number
L_c	length of the evaporator
L_c	length of the condenser
L_a	length of the adiabatic section
R_v	inner radius of the pipe
R_i	outer radius of the pipe without insulation
R_0	outer radius of the pipe with insulation
Re_z	axial Reynolds number
L_{eff}	effective length of heat pipe
K	wick permeability
$\Delta p\perp$	hydrostatic pressure drop
$\Delta p_{\parallel}$	axial hydrostatic pressure drop
F_l	liquid frictional coefficient
F_v	vapor frictional coefficient

K_b	bend loss coefficients
De	Dean number
f_b	friction factor for bend
f_s	friction factor for the straight sections.
K_b	bend loss coefficient
L_b	length of bend

Chapter 1

Introduction

Heat pipes are highly conductive heat transfer devices. This is 200 times more effect from small copper rod. In many industrial applications heat emitting components require cooling with in a small space. A heat pipe, which uses the latent heat of the working fluid for the heat transfer over a small temperature drop. The heat pipes are different form according to the nature of the application.

1.1 HEAT PIPE

Gaugler R.S. initially investigated the heat pipe concept in 1942.The remarkable properties of the heat pipe became appreciated and serious development work took place after its independent invention by Grover G. M. in the early 1960's.

A heat pipe typically has high conductance, usually an order of magnitude higher than a metal conductor of similar specifications. It transfers heat from a source to a sink by means of cyclic evaporation and condensation of a working fluid. It uses the latent heat of vaporization of the working fluid to transfer heat. The heat pipe does not require any external energy to function and it has no moving parts. For the same heat load, a heat pipe has a very low temperature drop due to its high efficiency. However, unlike a metal conductor a heat pipe has a limit on the amount of heat it can transfer.

1.2 CONSTRUCTION

The basic heat pipe concept can be demonstrated by a simple tubular metal casing with a wick covering the inner surface. The wick is made of different materials and has been one of the most investigated aspects of heat pipes. It is usually made of a porous material. A grooved structure can also be used. A working fluid is vacuum-sealed in a pre-determined quantity. The working fluid inside can be any compound that has good wetting characteristics on the wick and is selected on the basis of working temperatures of the heat pipe. If kinetic pressure losses of the vapor and gravitation head losses are neglected the properties of the working fluid can be combined to form a figure of merit M. The merit number determines the maximum possible heat transport using the heat pipe.

1.3   OPERATION

A heat pipe is broadly divided in three sections namely, evaporator, adiabatic and condenser. A typical heat pipe as shown in Figure has one evaporator section that takes heat from a source. The heat absorbed in the evaporator causes change of phase of the working fluid from liquid to vapor. The increased vapor pressure in the evaporator causes the vapor to exit from the evaporator section and travel through the adiabatic section. Traveling through the adiabatic section the vapor reaches the condenser region where condensation rejects the latent heat of the fluid to the sink. The condensed liquid is pumped back against an adverse pressure gradient to the evaporator by a combination of the capillary pumping action and/or bulk forces. This fluid circuit is repeated during the normal operation of the heat pipe and can continue as long as there is sufficient vapor pressure and capillary pressure to support its operation.

At the evaporator end the liquid recedes into the wick pores and hence the menisci in the pores at the vapor interface are highly curved. Whereas the liquid menisci at vapor interface in the condenser end are almost flat. This difference in the interface curvature of the menisci at the vapor interface coupled with the surface tension of the working fluid causes a capillary pressure gradient at the liquid-vapor interface along the length of the pipe. This capillary pressure gradient pumps the working fluid against various pressure losses such as friction, inertia and against bulk body forces. This axial variation of pressure is illustrated in Figure 1.1
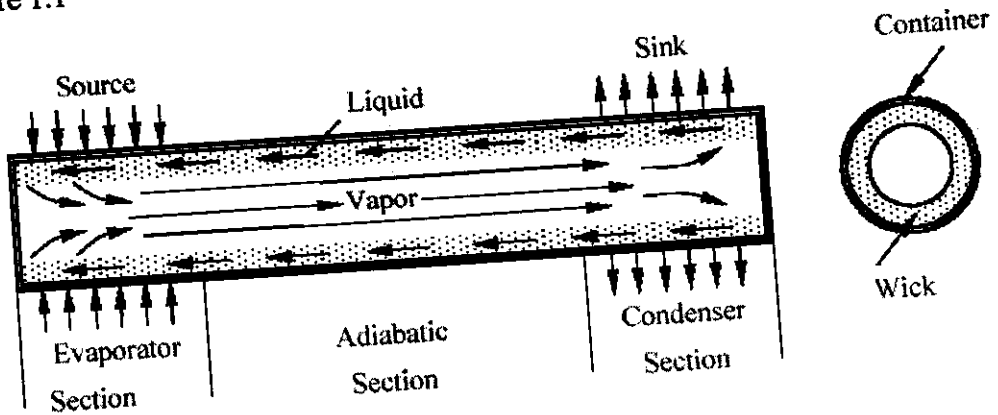
FIG.1.1: SCHEMATIC OF CONSTRUCTION AND
OF A TYPICAL HEAT PIPE
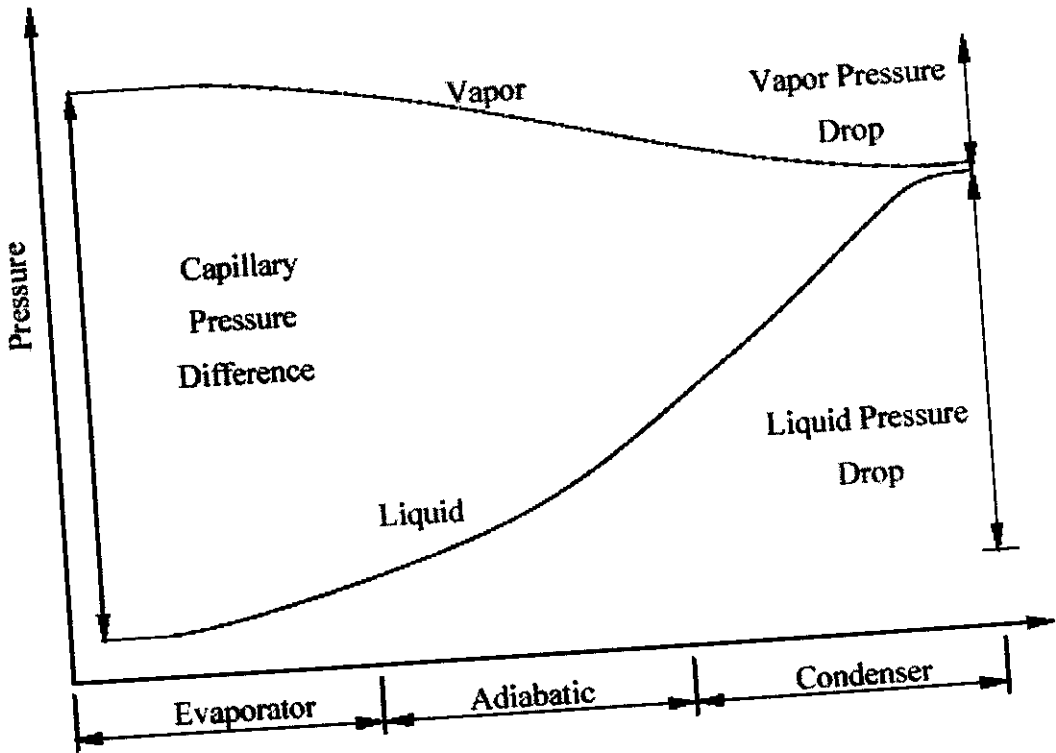
FIG.1.2: PRESSURE VARIATION ALONG A HEAT PIPE

1.4 OPERATING LIMITS

As with any other system, the performance and operation of a heat pipe is limited by various parameters. Physical phenomena that might limit heat transport in heat pipes include capillary forces, choked flow, interfacial shear and incipient boiling. The heat transfer limitations depend on the size and shape of the pipe, working fluid, wick parameters, and operating temperature. The lowest limit among these constraints defines the maximum heat transport limitation of a heat pipe at a given temperature.

1.4.1 Capillary Action

The difference in the capillary pressure across the liquid-vapor interfaces governs the operation of the heat pipes. This is one of the most important parameters that affect the performance and operation of a heat pipe. It is usually a major limiting factor in the working of low-temperature heat pipes. The capillary

The physical structure of the wick is one of the most important reasons for this limit and the type of working fluid also affects it. Once limit is encountered, any further increase in heat input may cause serious damage to the heat pipe.

When a heat pipe is operating in steady state, there is a continuous flow of vapor from the evaporator section to the condenser section and liquid from the condenser section to the evaporator section through the wick. These flows are possible because of the vapor pressure gradient (Δp_v) and the liquid pressure gradient (Δp_l) along the length of the heat pipe. There exists a capillary pressure due to the menisci formed at the liquid-vapor interface; this capillary pressure ($\Delta p_{cap,\,max}$) is necessary for the flow of liquid back to the evaporator. In addition, there are pressure gradients due to phase change taking place at the evaporator ($\Delta p_{e,\,phase}$) and the condenser ($\Delta p_{c,\,phase}$) ends and due to gravity (Δp_g). The capillary limit is expressed as,

$$\Delta p_{cap,max} \geq \Delta p_l + \Delta p_v + \Delta p_{e,phase} + \Delta p_{c,phase} + \Delta p_g$$

For the heat pipe to work normally, the capillary pressure should be greater than all the pressure gradients across the liquid-vapor path.

1.4.2 Sonic Limit

The evaporator and condenser sections of the heat pipe undergo addition and removal of mass due to the circulation of the working fluid. They act like a nozzle where vapor flows from the adiabatic section into or out of the end sections. The converging diverging nozzle like nature of the vapor flow path imposes a choking flow condition on the vapor velocity. The velocity at a choke point cannot be greater than the local speed of sound. This is called the sonic limit and the heat transfer can now only increase by increasing the operating temperature of the heat pipe. Although, the operation of a heat pipe under such condition causes a substantial temperature drop across the heat pipe, it is not considered a serious risk.

1.4.3 Boiling Limit

A typical cylindrical heat pipe receives heat at the evaporator end where it is transferred to the working fluid radically. When the input flux is sufficient, nucleation sites are formed inside the wick and bubbles are trapped in the wick, blocking liquid return that results in evaporator dry out. As compared to other heat pipe limits, boiling limit is a radial flux constraint and not an axial flux constraint. For liquid-metal heat pipes, the boiling limit is not very common.

1.4.4 Entrainment Limit

As liquid and vapor move in opposite directions, the vapor exerts a shearing force on the liquid at the liquid-vapor interface. If this shear force exceeds the surface tension of the liquid, liquid droplets are entrained into the vapor flow and are carried towards the condenser section. The magnitude of this shear force depends on the thermo-physical properties of the vapor and its velocity and if it becomes large enough, it causes dry out of the evaporator.

1.4.5 Viscous Limit

At low temperatures or low vapor densities, the viscosity of the vapor flow may be dominant as the flow progresses towards the condenser end. If the vapor pressure in the condenser is very low then the heat transfer under such a condition is limited. This usually occurs during the startup phase of a heat pipe.

1.4.6 Condenser Limit

For proper working of a heat pipe it is necessary that the heat be removed from the condenser end at the same rate as it is being added at the evaporator end. If non-condensable gases are accumulated at the condenser end, they reduce the working length of the condenser end, limiting the heat removing capacity of the condenser. This limit increases the possibility of capillary limit.
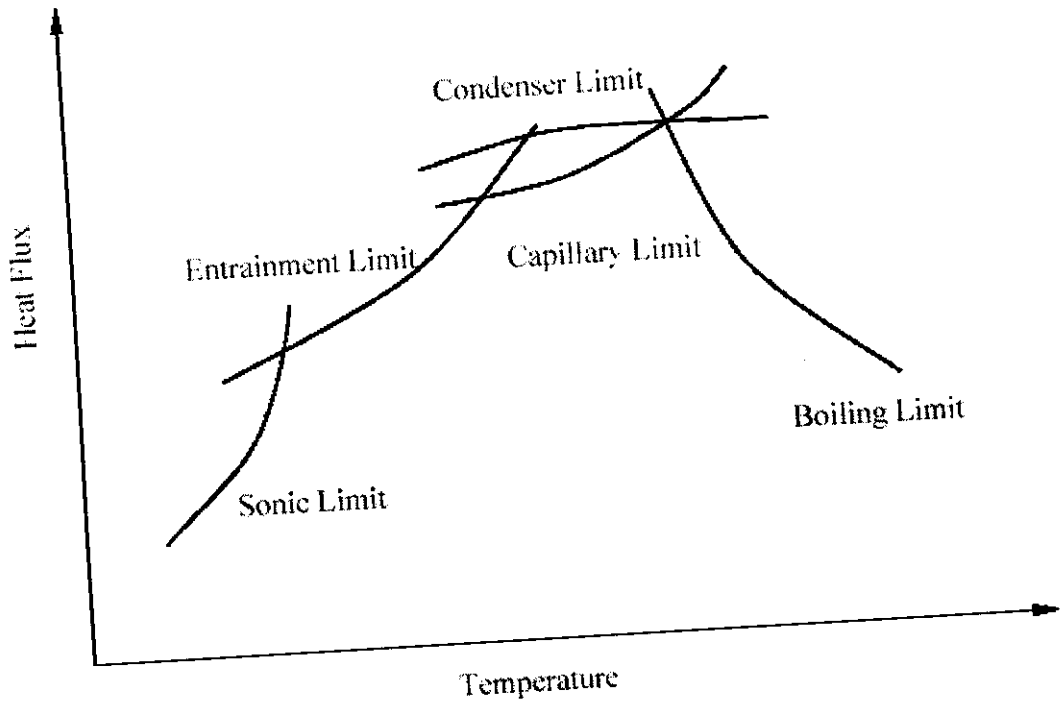
FIG.1.3: OPERATING LIMITS FOR A HEAT PIPE

Chapter 2

Literature Review

A capillary pumped heat pipe is one of the most efficient and yet very simple methods of heat transfer. A typical heat pipe is a cylindrical straight pipe, which is easy to fabricate and has a low cost of production. But in practice there is seldom any space available that can accommodate a straight heat pipe. The size of a heat pipe usually depends on the heat load it is subjected to. The lack of enough space demands a heat pipe that can be flexed to fit in available pockets of space in a system. Also it allows for compact and flexible overall system design.

Typical applications of heat pipes include desktop and laptop computers, transmission and engine cooling systems in automobiles. Other electronic components like circuit boards, transformers and power supplies are also common applications. The ever-reducing size of computers, electronic instruments and automobiles puts severe restrictions on the physical dimensions of heat pipes. Even when a heat pipe is not required in contorted configurations, the flexibility allows for misalignment between source and sink due to operational vibrations or oscillations.

As with the rest of the heat pipes, flexible heat pipes have received regular attention over the years and not surprisingly many of the problems were put forth by the aerospace industry. A thorough literature review is presented to summarize the previous work done in this area. Also, since the focus of this study is bent heat pipes, only portions pertaining to these types of heat pipes are covered.

2.1 REVIEW

A flexible heat pipe was developed and built by Bliss, Clark and Stein to analyze its operating characteristics for varying degrees of bend and under vibration in an unbent mode [2] .The purpose of this study was to design a flexible heat pipe capable of being bent or flexed during its operation allowing efficient heat transfer between an oscillating heat source and a stationary sink. The heat pipe was built using a rigid evaporator and condenser sections made from thick drawn copper tubing. A flexible adiabatic section fabricated from a seamless brass ____ _____ _____ them. A wick made of four layers of 150 mesh type 304

spring. It was tested for bends of 0°, 45° and 90° during horizontal operation and also at inclined orientations. The authors noted that the tests for various bends demonstrated an increase in the maximum heat flux associated with wick dry out after each flexing. It was speculated that this was due to the changes in the capillary passage between the layers of screen and wall as the heat pipe was flexed.

One interesting aspect of this study was the internal fin present in the condenser section. It was noted that since the fins significantly reduced the difference between the vapor temperature and the outside temperature of the condenser wall, it had greatly improved the operating efficiency of the heat pipe. The study concluded that the degree of bending had a minimal effect on the working of the heat pipe and a flexible heat pipe is a feasible idea.

Basiulis and Hummel investigated heat pipe techniques and their applications for electronic component cooling. The various techniques considered were heat pipes, cold plates, gas buffered heat pipes and unidirectional heat pipes. The flexible heat pipes provided relative motion between the heat source and heat sink [1]. This publication steps through the design process starting with the selection of a working fluid. The authors listed various applications for each type of heat pipes studied.

Edelstein designed and fabricated a variable conductance heat pipe radiator capable of passively controlling Freon-21 fluid loop temperatures under varying loads [4]. It was made from six-grooved heat pipes attached to an aluminum panel. The heat pipes had a flexible section that could bend up to 90°. Tests were carried out with radiator loads up to 800 W.

Saaski and Wright described a proof of concept for a flexible cryogenic heat pipe designed for space operations [20]. This heat pipe was meant for transmitting parasitic heat and generated heat from an infrared sensor on a satellite systems, a U shaped configuration of heat pipes is ...tions at 100 K was

bending. A multiple artery structure developed by McDonnell Douglas Astronautics Corporation (MDAC) was chosen due to its considerable capacity for bending. The artery was composed of a tightly wrapped bundle of many fine tubes, each of which functions independently as an artery to assure redundancy of fluid transport. The composite tube structure allowed for flexibility because each small tube could move independently to some degree. The evaporator and condenser were rigid sections connected by an adiabatic section made from bellows as shown in figure2.1. Thermal performance tests were carried out with R-21 at 293 K and methane at 100 K with the heat pipe in horizontal orientation and U shape configuration. The test results for both straight and bent mode were compared and it was concluded that there was no significant effect due to bending.

A comprehensive test program was executed to determine the physical and thermal performance of two flexible cryogenic heat pipes to provide an efficient and flexible thermal link between a detector and a space radiator by Wright et al. at Rockwell International Corp Space Division [24]. To determine the optimum geometry and materials for the container and the wick, parametric studies were performed and the 100 – 200 K pipe was designed with methane and ethane as the working fluid, with nitrogen and oxygen for the 15 – 100 K pipe. The wick selected was a multi wrap composite, which consisted of a spirally wrapped coarse mesh screen surrounded by a fine mesh outer wrap. V-groove screw threads were machined into the evaporator and condenser whereas a braided flexible bellows made from stainless steel was used for the adiabatic section. This flexible section together with the spiral multi wrap wick demonstrated good flexibility and compatibility with methane as the working fluid. The authors concluded that overall this configuration worked well as a highly flexible link between the sources and the sink and had good potential for high power transport scenarios.
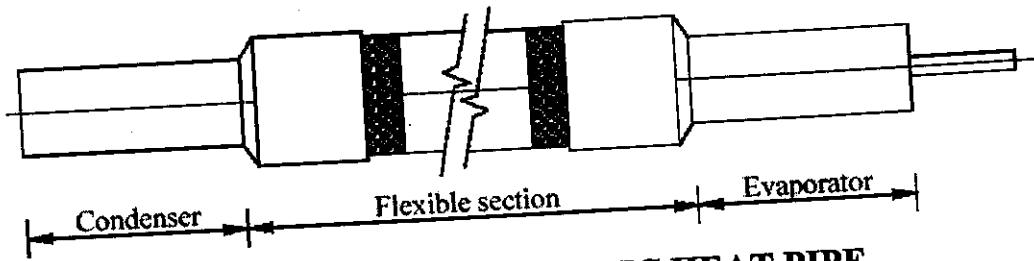
FIG.2.1: FLEXIBLE CRYOGENIC HEAT PIPE

Koch, Kreeb and Perdu developed a modular axial grooved heat pipe system for an operating temperature range of 100 – 400 K intended for typical space applications [12]. Various tests were performed to evaluate the performance as a function of temperature or inclination angle, start up, operating life, working fluid and of bended heat pipes.

Munzel et al. conducted an experiment for the European Space Research and Technology that consisted of two bendable artery heat pipes which were flown aboard a rocket Centre as a part of the International Heat Pipe Experiment [16] .It consisted of two aluminum heat pipes having a length of about 90 cm with an outer diameter of 0.7cm. The wick and artery systems were made from 160 mesh stainless steel screen and ammonia was the intended working fluid. The two arteries were positioned to lie in the same diametric plane so that the pipes could be bent with no reduction in the heat transport capability. The experiment was supposed to test two heat pipes; one straight and one bent into a z-shape. The bent heat pipe was later replaced with a straight one due to priming problems.

There is growing interest in heat pipe thermal diodes and thermal switches for space applications. A thermal diode can protect electronic components from overheating during mission critical periods like pre launch operations, vehicle maneuvers and reentry into the earth's atmosphere [8]. Similarly, a thermal switch can be used for transport of heat from a source to one of several heat sinks depending on the operating conditions.

Croll et al. undertook for development work near room temperature

predict the transient shutdown of the thermal diode using a mathematical model and experimental results, both of which were in good agreement. It was noted that bend ability is no serious constraint for all three designs, though in the case of complex artery structures, e.g. modular artery with 4 or 5 webs, the bend radius has to be relatively large to avoid performance degradations.

Peeples fabricated three variable conductance heat pipes and Calhoun in order to investigate the effect of tight radius bends in the adiabatic section on the heat pipe performance [17]. Analytical studies were conducted to evaluate the geometry and performance requirements of candidate heat pipe designs. The heat pipes were bent in the adiabatic section to make a J or L shape with a very small bend radius. There was a probability that capillary pumping could be reduced due to deformation of internal structure in the bent area, resulting in performance degradation. Two pipes were fabricated from a thin wall stainless steel with a multi-tube central artery and a wall screen wick. Freon 21 was the working fluid. The third pipe was made of aluminum with an axially grooved wick and ammonia was used as the working fluid. All the pipes were bent using a conventional pipe bender and it was found using a radiograph image that in the bent area the deformation of the artery lowered the permeability of artery, effectively reducing the heat transfer capacity of the pipe due to inadequate flow of condensate from condenser to evaporator. The corrugations in the inner bend surfaces of the heat pipe tube, and local separation of the wall wick, caused unpredictable voids and it also made it difficult to determine the exact charge of the working fluid required. In order to circumvent these problems, the heat pipes were fabricated in such a way that the heat pipe tube was bent before inserting the wick structure and also wick in the bent area was removed to minimize cavities caused..

A bendable gas controlled variable conductance heat pipe was developed and made entirely from stainless steel with ammonia as working fluid and a homogeneous wick as capillary system [13] designed by Mathieu et al. It presented an excellent potential for high performance because of its heat transport capability of 100 W through a 1 cm diameter tube. There were performance

presence of control gas (variable conductance) and, the heat pipe should not lose any performance when curved in U-shape with a radius of curvature of 10 cm.

Meier et al. designed a heat pipe for use in a space reactor where it was required to bend around the reactor core in two approximately 90° bends on a 180 mm radius and have design lifetime of 7 years [18]. Because of this lifetime requirement and working temperature of 1400 K, molybdenum was the material chosen for the container with sodium as the compatible working fluid. It employed a non-concentric screen annular sintered wick. Before fabrication of the heat pipe, a series of bending experiments were carried out to finalize proper bending procedure and temperature so that no cracks or breaks were generated. A bending test when conducted on an unsupported wick at 353 K that showed the compression side of the bent wick was severely buckled. The buckles caused a reduction of 17% in the vapor flow area and an increase in pore size was also observed at the sharp corners, which would lead to significant reduction in performance.

The conclusion was that bending on an unsupported wick would not produce satisfactory results. Another bending test with a steel tube mandrel to prevent buckling of the wick was performed, but large tears were generated on the tension side. Finally, a stainless steel heat pipe was completely filled with sodium at 1070 K. When the pipe was bent at 365 K (highest attainable temperature to provide required ductility for molybdenum but still low enough to keep the sodium mandrel in solid state), the results were successful with no tears in the tension side and very little buckling on the compression side with a very minute change in porosity.
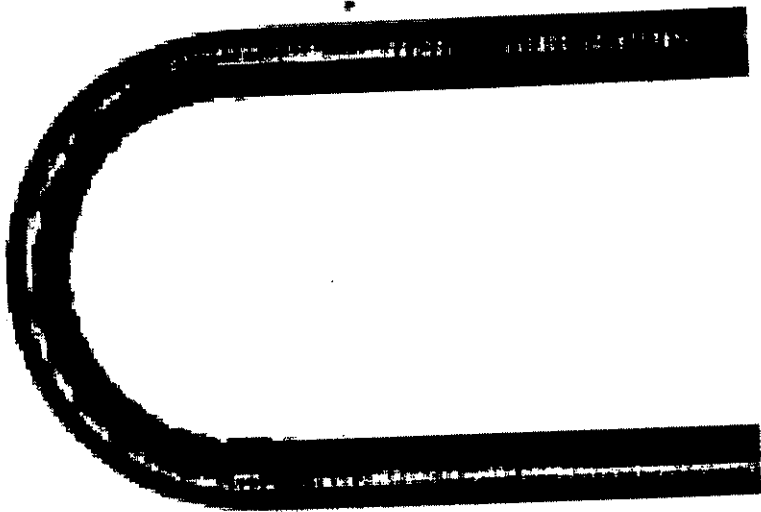
(a) CONVENTIONAL WICK STRUCTURE
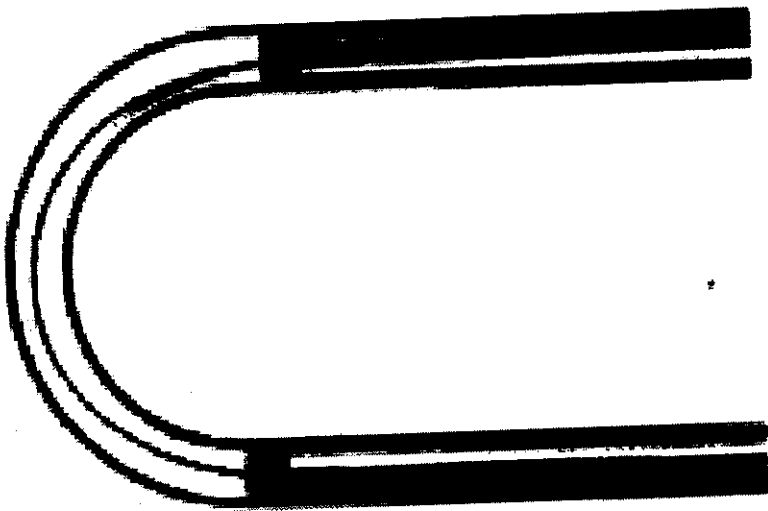
(b) MODIFIED WICK STRUCTURE

FIG.2.2: HEAT PIPE BENDS

Ernst in a report to NASA JPL for a heat pipe heat rejection system and demonstration model for the nuclear electric propulsion (NEP) spacecraft evaluated and redesigned prototype heat pipe components, and then further fabricated and tested them [5]. The evaluation demonstrated the validity of several complicated geometries and wick structures including bends in the heat pipe. Two types of heat pipes with 30° bends at each end of the adiabatic section were tested for several wick designs. A heat pipe with our wraps of 325-mesh wick was found

as a good design with respect to performance and mass. It transferred 3800 W over a temperature drop of 117.9°C.

Merrigan et al. demonstrated in a 1984 publication that flexible sodium/stainless steel heat pipes can be fabricated and operated at temperatures up to 1100 K with an axial heat flux of 1950 W/cm². The relevance of this publication to the work in this thesis is the study of the effect of bend angle on the heat pipe temperature distribution. There was a requirement for high power, flexible heat pipe capable of bending through angles of up to 180° and working temperatures of both cold and high temperatures. Therefore, as a demonstration flexible heat pipe employing sodium as working fluid and using stainless steel wick and tube was fabricated and tested. "This device has been flexed repeatedly through angles of 180°, both at room temperature with the sodium working fluid frozen and at temperatures to 1000 K while radiating heat to a room temperature environment". A 100-mesh stainless steel screen wrapped in 3 layers in alternating directions was used to make the wick. The adiabatic section was made from a standard high vacuum flexible line section. The heat pipe was tested at a temperature of 1000 K in the horizontal orientation. Then the condenser end was elevated upward through an arc up to a bend of 180° in the vertical plane. The heat pipe operation was visually verified during this bending experiment.

Later to determine the effect of bending on the performance, the heat pipe was operated in the horizontal position and tested in three positions of 0°, 90° and 180°. During testing axial temperatures were recorded against input power to the heat pipe (Figure2.3) shows the results of these experiments. While the data indicates a significant increase in axial temperature drop, there was no loss of heat pipe function due to bending even under test loads up to 1950 W/cm². Repeated startup tests were conducted from below the freezing point of sodium (working fluid) with no apparent effect due to bending. The authors concluded that this heat pipe could be bent up to 180° even when under load.

Shaubach and Gernert worked on a project to develop and demonstrate flexible heat pipes for transport of heat from stationary to translating sections of

with a screen wick that allowed bending. Such heat pipes are typically low power devices due to the high flow resistance of the screen wick structure.
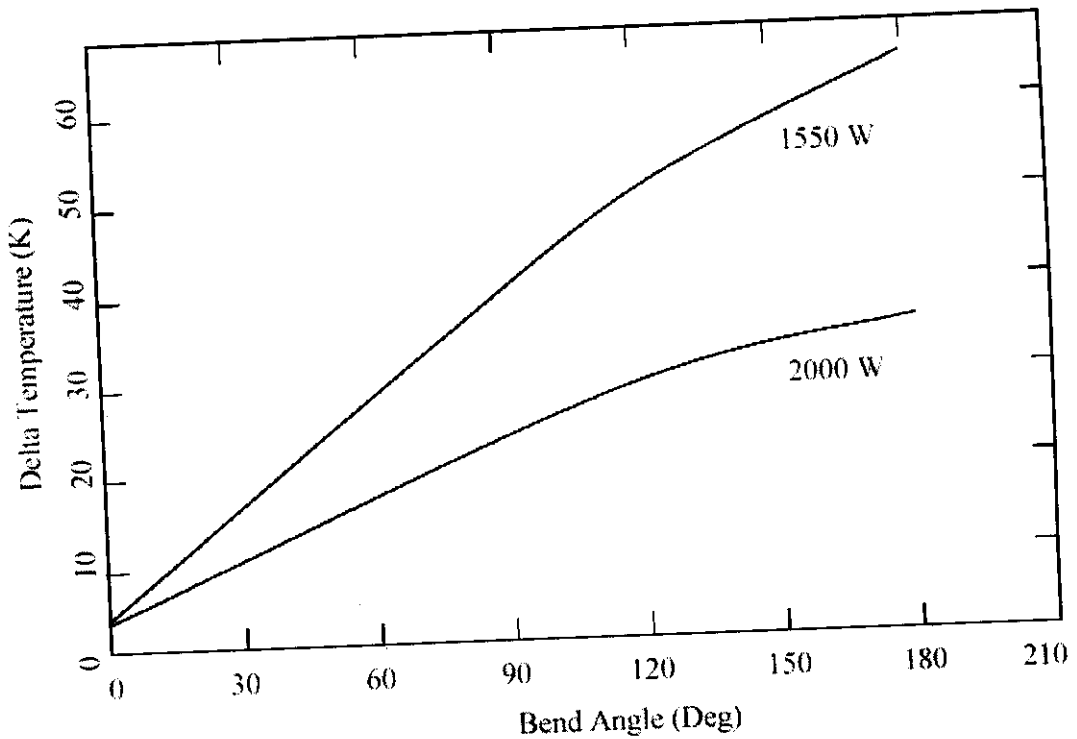
FIG.2.3: ΔT BETWEEN EVAPORATOR EXIT AND END OF CONDENSER VERSUS BEND ANGLE OF HEAT PIPE

Flexible heat pipes with high power capacity are made possible by using flexible screen arteries, which can be made from several different alloys and mesh sizes. These flexible screen arteries are integrated with high performance circumferential distribution wicks in an envelope that is flexible in the adiabatic section. Three heat pipes identical in all respects except that the wicks were built using screens, powder metal and spiral "V" grooves were tested. A computer program developed at Thermacore Inc. was used to estimate the performance of each heat pipe; these calculations showed that for the same power the lowest ΔT was predicted for the heat pipe with the microgrooves followed by the sintered powder metal and the wrap screen, whereas the sintered powder metal wick had the highest predicted heat transport capability followed by the wrapped screen wick and then the microgrooves. The microgrooves design was dropped due to difficulties faced in fabrication. The better performance obtained with sintered

powder wicks as compared to the screen a wick was attributed to the bonding of wick structure to the heat pipe wall. A screen wick has empty clearances between the layers and gap between the screen and the heat pipe wall. These clearances are filled with a comparatively low thermal conductivity working fluid that increases the thermal resistance of the heat pipe and consequently causes increase in the temperature drop. This difference causes an increase in performance by a factor of 3 in sintered powder wicks.

Hwangbo and Joost developed a variable conductance heat pipe with a flexible joint for temperature control of high power electronics using a space radiator [10] .The design requirements for this pipe mandated that a 0.5" O.D. heat pipe should be able to sustain loads up to 3500 W-inch at a vapor temperature of 80 °F. The design consisted of a sintered screen axial slab made by a 20-mesh screen sandwiched between two 100-mesh screens. This benefited from the increased permeability due to the 20-mesh screen as well as better capillary pumping by the 100 mesh screens. An analytical model was developed and several operating conditions were simulated to demonstrate the feasibility of this design with ammonia as working fluid.

Peterson [18] developed a bellows heat pipe using analytical and computer modeling for cooling of electronic components. This study first developed an analytical model that was used to build a computer model. Since the design of the heat pipe was governed by the evaporator temperature i.e. temperature of electronic component, the source heat flux was not specified in the model. The results from the computer model were benchmarked against previous work in this field and were found to agree with the results obtained by others. This computer model was then used for designing and optimizing a bellows heat pipe, which was designed to maintain the heat source at a constant temperature of 40°C. It is noted that this heat pipe was capable of transporting 45 W with a thermal resistance of 0.47°C/W.

A flexible loop heat pipe cold Gernert and Brown developed plate [7]. The major

difference is that this prototype operates in any orientation. It sustained a heat load of 45 W over a temperature drop of 20 °C.

The Advanced Camera for Surveys (ACS) is an instrument containing two CCD cameras. It operates at temperatures below -80 °C. Using two thermo-electric coolers, which transported the heat from the cameras to heat pipes, which in turn transported it to the sink, cooled the camera. The heat pipes were chosen since they are frequently used in space applications for passive heat transport to remotely and awkwardly located radiator panels. Since the location and alignment of the CCDs were important, the heat pipes were designed with a flexible section to minimize the thermal induced structural loads. This work by Schweickart and Buchko discussed the design and testing of these heat pipes. The flexible heat pipes used ammonia as working fluid and a rolled screen mesh wick supported by screen mesh web. Both the evaporator and condenser were 316L stainless steel and the flexible section was made from Swagelok® flexible stainless steel hose. As the flexible sections of the heat pipes were pre-formed after the wicks were inserted, additional bending of the flexible section posed little risk of wick damage. Thermal performance testing showed that both pipes exceeded their minimum required heat transport capacity by a wide margin.

In an effort to build a flexible heat pipe that can provide for bending, twisting, oscillating and deforming that is typically required in compact electronics, Lu Shaoning and Li His-Shang designed and built prototypes of a mini flexible heat pipe with a vacuum grade transparent plastic tube [21]. The heat pipes were small in diameter, typically few millimeters, so as to accommodate mobile computers. New wick structures were designed to make internal two-phase flow visible while providing the required capillary pumping action. The evaporator and condenser of the heat pipes were made of brass tubes and a transparent polyurethane tube was used for the flexible adiabatic transport section. Transparent wick structures were built from copper wire spring with a spring-braid wick and helical mesh stripe. This work however only discussed results from spring wick heat pipe that made good contact with the heat pipe container ... flexibility was maintained in any bent position. The spring was made from

Ultra-high-molecular-weight (UHMW) film wicks and formed UHMW wicks with Kapton and aluminized Mylar containers were used to design, fabricate and test flexible heat pipes by Glass et al. The heat pipes used methanol as the working fluid and tests were carried out at steady state. The authors note "The successful fabrication and operation of the heat pipe demonstrated that flexible polymeric heat pipes are feasible. From preliminary design studies, it appears that the design of a wick such that capillary and boiling limits are satisfied is the primary challenge".

Muenzel discusses test results for life tests of heat pipes used in a telecommunications satellite with the test setup in a report for ESA [15]. Four bendable artery heat pipes 7 mm in diameter were subjected to life tests under a variety of operating conditions, both stationary and accelerated as well as under thermal shocks.

Ernst and Eastman studied designs for liquid metal heat pipes for space and terrestrial applications for high temperature heat recovery [5] .The design criterion and several wick designs like sintered powder wick/arteries, sintered axial grooves and flexible screen arteries were discussed.

. Bhatti and Vanoost considered A95 stainless steel heat pipes with ammonia as working fluid for all possible cases of space applications. Different bend configurations and lengths were also included in the study.

A flexible heat pipe cold plate technology was developed by Gernet at al for aircraft thermal control [7]. Four such heat pipes were built for a variety of difficult aircraft cooling situations. In each case, a cold plate transferred the source heat to the most convenient heat sink by an integrally connected flexible heat pipe. This permitted relative motion between the electronics package to be cooled and the heat sink and it also allowed cooling system access in awkward places.

A method was suggested by Gus'kov et al. suggested a method for

permitted prediction of the heat pipe operation with various working fluids and different design variations; one such result for propylene heat pipe was presented.

A report of joint activities of various Russian organizations aimed at the development of a flexible heat pipe and its modified version intended for thermal management of spacecraft instrumentation was presented by Zelenov at al [25] .A flexible heat pipe increased reliability of units moving, folding and opening in space in addition to a reduction in power consumption of the thermal control system. Different heat pipes were developed as an outcome of experimental and theoretical studies of various configurations of the evaporator, condenser and adiabatic zones. It was shown that the principal performance characteristics of these pipes were comparable to other flexible heat pipes' performance.

Chapter 3

Factors Affecting Design and Performance

3.1 INTRODUCTION

As described before, the basic components of a heat pipe are the working fluid, the container and the capillary structure. During the construction of a heat pipe a number of factors control the type of materials that can be used. Also, it is obvious that there will be some conflicting combinations that will not work when used in a heat pipe.

3.2 WORKING FLUID

Every heat pipe is designed for a particular operating temperature range. The selection of the working fluid mainly depends on this range of temperatures. Some of the commonly used working fluids in AuTherMML are listed in Table along with their related thermo physical properties and useful ranges. The useful range of a working fluid extends from the point where the saturation pressure is greater than 0.1 atm and less than 20 atm

Within the operating temperature range, a variety of possible fluids can be used. In order to determine the best working fluid, a number of characteristics must be examined. The main characteristics are discussed in following pages

TABLE 3.1: THERMO PHYSICAL PROPERTIES OF WORKING FLUIDS

Working Fluid	Melting Point, K at 1 atm	Boiling Point, K at 1 atm	Useful Range, K
Water	273.1	373.1	303 – 473
Methanol	175.1	337.8	283 – 403
R134a	172.0	246.4	208 – 343

3.2.1 Compatibility with Wick and Container

Chemical compatibility of the heat pipe container metal and the working

~~d the container might work as a galvanic~~

cell in tandem with other parts of the heat pipe. Any such reaction may generate non-condensable gases degrading the overall performance of the heat pipe.

3.2.2 Thermal Stability

At working temperatures that are typically higher than room temperatures, the container metal may act as a catalyst in decomposition of the working fluid. Some organic fluids break down into different compounds necessitating the need to keep the film temperature below certain temperatures. This is not a problem for inorganic fluids.

3.2.3 Wetting of Wick and Container

Any fluid can be used in a conventional heat pipe provided it has good wetting characteristics with the wick and container wall material. The capillary pressure generated in the wick is subject to wet ability of the fluid with the wick structure. Also, good wetting can increase the superheat required to initiate boiling. When a fluid does not have good wetting characteristic, it can be improved by surface treatments. To improve wetting characteristics, the copper containers were oxidized during fabrication of the heat pipes used in this research.

3.2.4 High Latent Heat and Thermal Conductivity

The heat transport through the heat pipe is a direct function of the latent heat of the working fluid. The performance of the heat pipe is directly proportional to the latent heat. Also, a higher latent heat allows for good heat transfer at lower temperatures. Thermal conductivity of the working fluid is of major concern at the condenser end. The condensed liquid has a comparatively lower conductivity and increased thermal resistance.

3.3 CONTAINER

The function of the container is to provide a hermetically sealed enclosure for the working fluid. It is necessary to avoid any diffusion of air into the heat pipe. The type of the heat pipe and its application decides the shape of the

compatibility, strength to weight ratio, thermal conductivity, ease of machining and wet ability.

Degradation of the container material leads to chemical reaction with the working fluid. In addition to generating non-condensable, these reactions tend to corrode the internal surfaces of the container, increasing the thermal resistance and also reducing the surface tension and wetting angle. Such chemical reactions also cause pitting of the inside wall that promotes formation of enhanced nucleation sites which leads to premature boiling of the working fluid.

Apart from the chemical compatibility, a heat pipe container is necessarily a pressure vessel and hence careful attention is required for selection of material grade. Also, it is required to make a leak proof seal and structural integrity must be ensured for the entire working pressure range of the heat pipe.
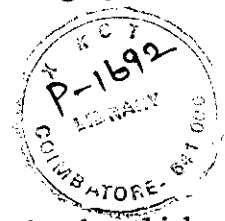
3.4   CAPILLARY STRUCTURE

The capillary wick structure in a heat pipe provides a mechanism by which the working fluid returns to the evaporator and evenly distributes the liquid film over the evaporator surface on the inside. Since the capillary force is of premier importance to sustain the working of heat pipes, the wick pores must be small. Smaller pores provide for greater capillary pumping pressure but also increase resistance to liquid flow through the wick, thereby increasing the overall liquid pressure drop across the wick. The wick covers the entire inner surface of the heat pipe and hence, the heat must travel through heat pipe container walls and wick to evaporate the liquid. The radial temperature drop due to this is dependent on the thickness of the wick and its thermal conductivity. For a higher thermal conductivity the wick must have lower porosity but this conflicts with the need for lower liquid pressure gradient .The wick structures are broadly classified into two categories as discussed in following sections.

3.4.1 Homogeneous Wicks

Homogeneous wicks are constructed from a single material that has a uniform cross section. The common materials used include metal screens, sintered

of wick made from these materials has its own advantages and limitations, and a detailed discussion on this topic is beyond the scope of this work.

3.4.2 Composite Wicks

A composite wicking structure is built using two or more materials described in section 3.4.1 thus taking advantage of their respective strengths. A composite wick typically handles the two main functions of capillary pumping and liquid transport in different sections of the wick. A typical example is a screen wick covering the axially grooved wick structure as shown in Figure
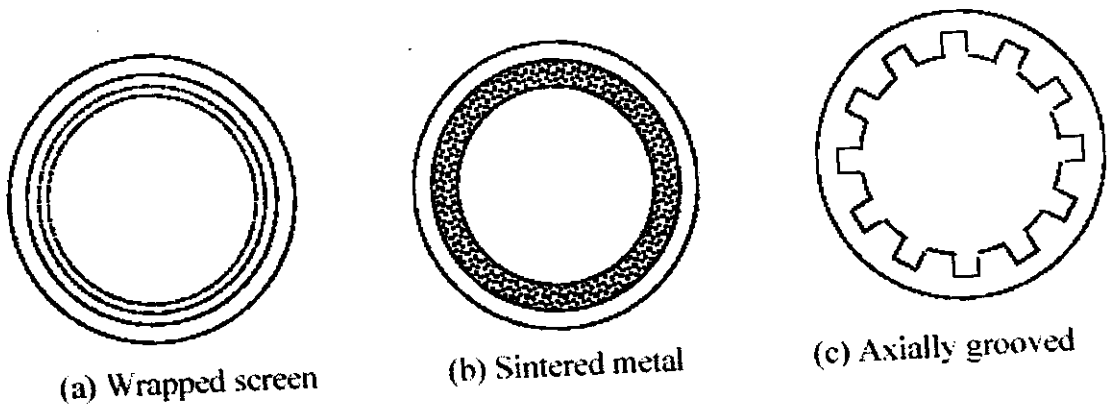

| (a) Wrapped screen | (b) Sintered metal | (c) Axially grooved |

FIG.3.1: HOMOGENEOUS WICKS

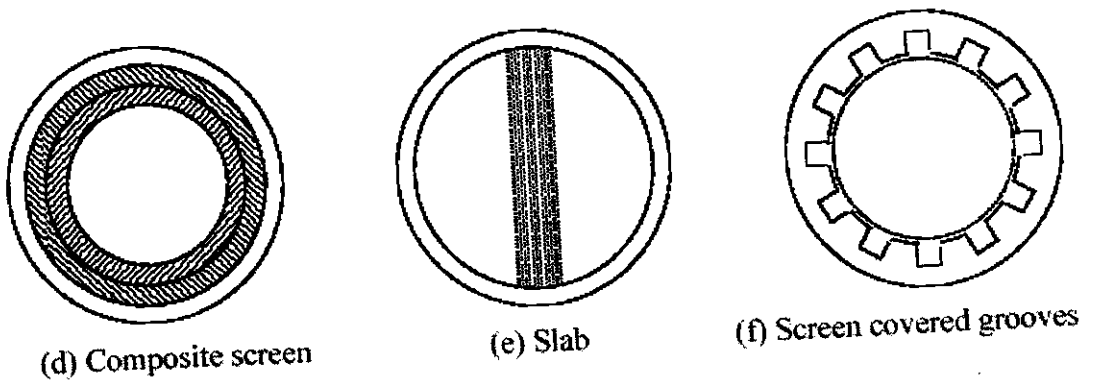| (d) Composite screen | (e) Slab | (f) Screen covered grooves |

FIG.3.2: COMPOSITE WICKS

Chapter 4

Bends in Heat Pipe

4.1 INTRODUCTION

As discussed in Chapter 2, flexible heat pipes have garnered significant research interest in the past due to their obvious advantages. Flexible heat pipe designs include flexible sections made from bellows or bendable tubing. These types of heat pipes are usually designed to be fabricated in a particular shape. Fabrication techniques were developed to make bended heat pipes in required shapes and in some cases wicks were totally removed from the flexible sections to avoid potential problems with deformed wicks.

It is observed that there are no references in the literature for heat pipes that can be bent into a contorted shape after fabrication. This thesis documents the evaluation and testing of bendable copper-water heat pipes made using sintered copper felt wicks. Once fabricated, this heat pipe can be twisted to fit into the available space or reach narrow spaces.

4.2 BENDABLE WICKS

Only certain types of wicks can be used in bendable heat pipes. And wick will have a tendency to separate from the container walls under bending. This separation has two adverse effects, a reduction in the vapor core area that reduces heat transfer capacity and a disruption in the path of liquid flowing back to the evaporator. If the bending angle is severe, the wick can crumple and even tear off in extreme cases. The sintered copper felt wick provides a very flexible wick material that does not crack after bending as well. However, a wick made from sintered metal powder will crack under bending. Although other wicks made from metal screens may also work with supporting springs, this work is a continuation of ongoing work on metal felt heat pipes at AuTherMML .

The heat pipe was bent in only one location to reduce the complexities in testing. After successful tests on such heat pipes further studies on multiple bends could be carried out. Several bending angles (15°, 30°, 45°, 60° and 90°)

A series of photographs of the heat pipe cross-section after bending were

observed. However, it was noted (Figure4.1) that the separation from the wall slowed down after 45°. Also a 90° bend was cut and, it was observed that the wick was not damaged due to stretching and crumpling at outer and inner walls as shown in Figure4.2 (a) & (b). It can be seen inFigure4.2 (c) - (e). that the inner and outer walls of the curved part of the heat pipe had deformed due to crumpling and stretching respectively. The working fluid gets trapped in the gaps created by the separation of the wick from the container walls. This film of working fluid has a lower conductivity as compared to that of the wick and it reduces the heat transfer to the heat pipe. Therefore, deformation is acceptable only in the adiabatic section and not in the condenser section and the evaporator section.
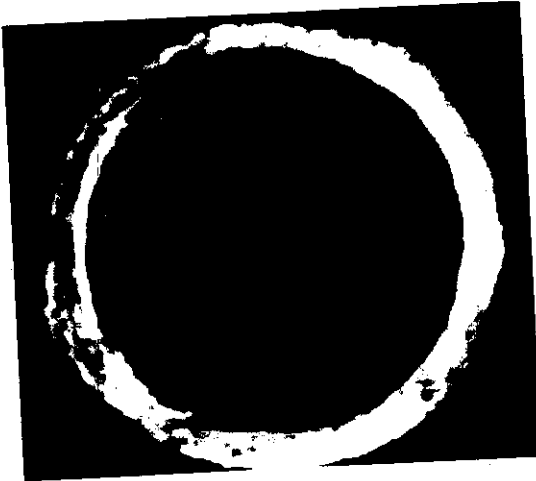
(a) Straight Heat Pipe
(10x magnification)
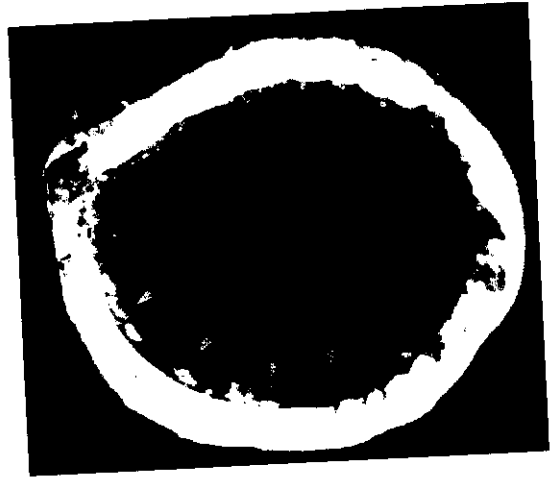
(b) 15° Bend
(10x magnification)

(c) 30° Bend
(10x magnification)

(d) 45° Bend
(10x magnification)

(e) 60° Bend
(10x magnification)

(f) 90° Bend
(10x magnification)

FIG.4.1: WICK SEPARATION NEAR HEAT PIPE WALL DUE TO BENDING

(a) No damage to wick (90°)
(10x magnification)
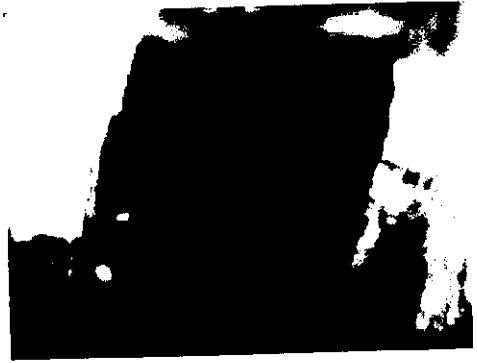
(b) No damage to wick (90°)
(10x magnification)
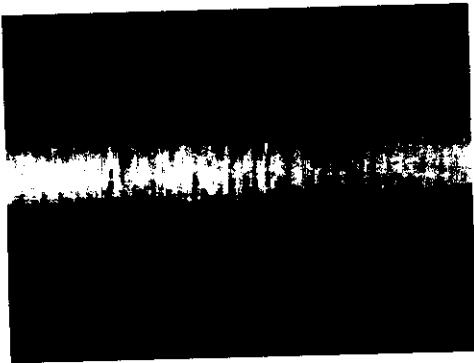
(c) Straight heat pipe wall texture
(5x magnification)

(d) Bended heat pipe inner wall
(5x magnification)
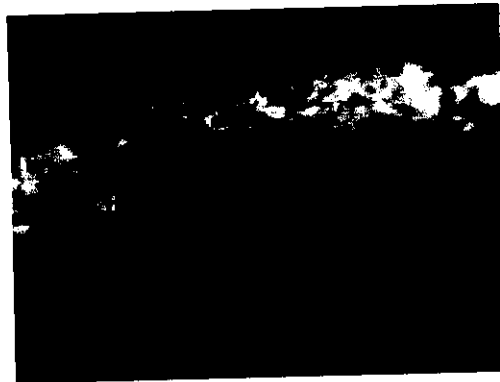
(e) Bended heat pipe outer wall
(5x magnification)

FIG.4.2: BENDING EFFECTS ON HEAT PIPE WALL &WICK

4.3   PERFORMANCE LIMIT

As discussed in Section 1.4, a heat pipe has various performance limits. However, when the heat pipe has a single bend at the center, the only limit affected is the capillary limit. As shown in Equation, the vapor pressure drop and liquid pressure drop will be affected due to bending as the flow paths are altered. Low fluid velocities typically characterize the liquid flow and bending effects can be neglected. Therefore, at steady mass flow, the vapor velocities are very high and the flow is laminar or turbulent depending on working temperature and heat load.

4.3.1   Vapor Pressure Drop

A detailed analysis of vapor flow bending effects on the capillary limit, The capillary limit is given by,

$$\Delta p_{cop,\max} \geq \Delta p_l + \Delta p_v + \Delta p_{e,phase} + \Delta p_{c,phase} + \Delta p_g \qquad (4.1)$$

The maximum capillary head is given by,

$$\Delta p_{cop,\max} = \frac{2\sigma}{r_{eff}} \qquad (4.2)$$

Where r_{eff} is the effective capillary radius and $\acute{o}$ is the surface tension. Busse assumed that the vapor flow was laminar and the heat pipe was isothermal, so density was constant. Also the axial pressure gradient was assumed constant over the heat pipe cross section. The two dimensional steady flow of the incompressible vapor is represented by the conservation equations for mass and momentum

r momentum equation:

$$v\frac{\partial v}{\partial r} + w\frac{\partial v}{\partial z} = -\frac{1}{\rho}\frac{\partial p}{\partial r} + v\left[\frac{\partial}{\partial r}\left(\frac{1}{r}\frac{\partial}{\partial r}(rv)\right) + \frac{\partial^2 v}{\partial z^2}\right] \qquad (4.3)$$

Z momentum equation:

$$v\frac{\partial w}{\partial r} + w\frac{\partial w}{\partial z} = -\frac{1}{\rho}\frac{\partial p}{\partial z} + \nu\left[\frac{1}{r}\frac{\partial}{\partial r}\left(r\frac{\partial w}{\partial r}\right) + \frac{\partial^2 v}{\partial z^2}\right] \qquad (4.4)$$

Continuity equation:

$$\frac{1}{r}\frac{\partial}{\partial r}(rv) + \frac{\partial w}{\partial z} = 0 \qquad (4.5)$$

Boundary conditions:

At r = 0

$$\frac{\partial w}{\partial r} = 0, v = 0 \qquad (4.6)$$

At r = R

$$w = 0, v = \begin{cases} v_s, 0 \leq z \leq L_e \\ 0, L_e \leq z \leq L_e + L_a \\ -v_s, L_e + L_a \leq z \leq L_t \end{cases}$$

A radial Reynolds number Re$_r$ is defined as vapor velocity distributions are related to interfacial velocity

$$\mathrm{Re}_r = \frac{\rho_v v_\delta R_V}{\mu_v} \qquad (4.7)$$

This is related to the rate of mass flow per unit length by,

$$\mathrm{Re}_r = \frac{1}{2\pi\mu_v}\frac{dm}{dz} \qquad (4.8)$$

To solve these equations, Busse proposed an approximate expression for the axial velocity profile,

$$(\ ,\ ) = 2w(z)\left(1 - \frac{r^2}{\ }\right)\left[1 + a(z)\left(\frac{r^2}{R^2} - \frac{1}{3}\right)\right] \qquad (4.9)$$

Where $a(z)$ is an arbitrary function for the correction to the parabolic Poiseuille velocity profile that was found by assuming that the average pressure gradient over the cross section equals the axial pressure gradient at the center .The values of $a(z)$ for various values of radial Reynolds numbers are shown in Figure. This gives results for the pressure drops in all three sections

Evaporator:

$$\Delta p_e = -\frac{8\mu_v Q_e}{\Pi \rho_v R_v^4 h_{fg}} \frac{L_C}{2}\left[1 + \mathrm{Re}_r\left(\frac{7}{9} - \frac{8A}{27} + \frac{23A^2}{405}\right)\right]$$ (4.10)

Adiabatic:

$$\Delta p_e = -\frac{8\mu_v Q_e}{\Pi \rho_v R_v^4 h_{fg}} L_a\left[1 + \frac{\mathrm{Re}_z R_v}{8L_a}\left(\frac{8(A-a)}{27} + \frac{23(A^2 - a^2)}{405}\right)\right]$$ (4.11)

Condenser:

$$\Delta p_e = -\frac{8\mu_v Q_e}{\Pi \rho_v R_v^4 h_{fg}} \frac{L_c}{2}\left[1 + \mathrm{Re}_r\left(\frac{7}{9} - \frac{8a}{27} + \frac{23a^2}{405}\right)\right]$$ (4.12)
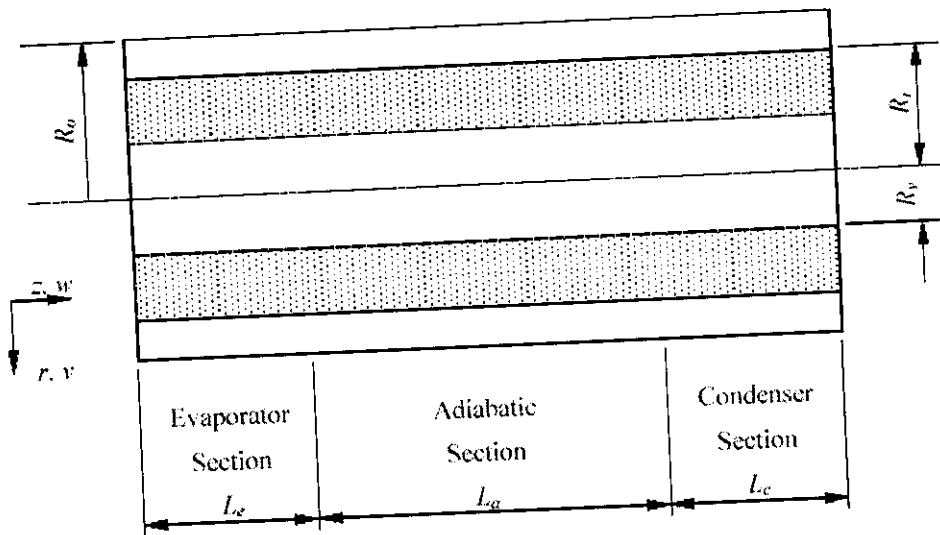
FIGURE 4.3: HEAT PIPE NOMENCLATURE
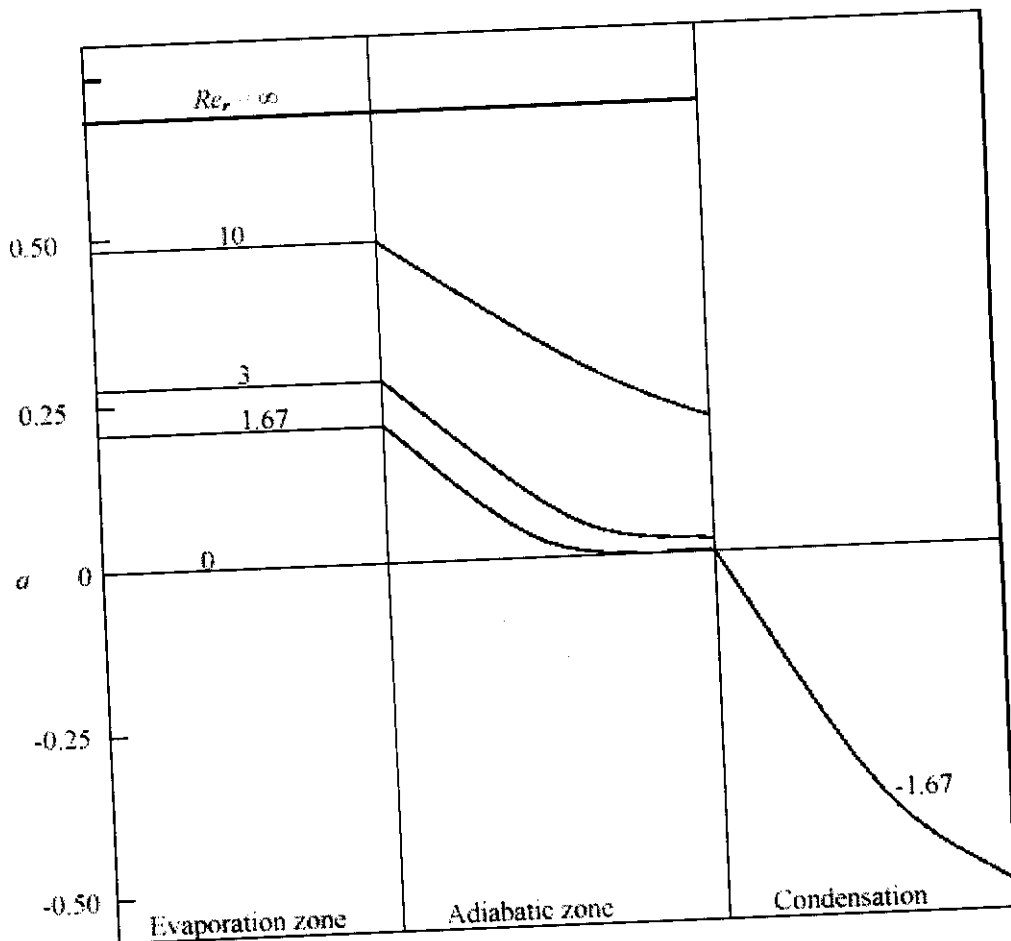
FIGURE 4.4: THE CORRECTION FUNCTION $a(Z)$

$$\text{Re}_r = \frac{1}{2\pi\mu_v}\frac{dm}{dz} \tag{4.13}$$

and A is

$$A = \frac{15}{22}\left[5+\frac{18}{\text{Re}_r}-\sqrt{\left(5\frac{18}{\text{Re}_r}\right)^2-\frac{44}{5}}\right] \tag{4.14}$$

For the case, when the wet point is near the condenser end cap the pressure drop in the entire heat pipe is found by adding Equations

$$\Delta p_v = -\frac{(f\,\text{Re}_z)\mu_v}{2R_v^4 A_v\rho_v h_{fg}}Q_e L_{eff} \tag{4.15}$$

where L_{eff} is the effective length of heat pipe,

$$L_{eff} = \frac{L_e}{2}+L_A+\frac{L_c}{2} \tag{4.16}$$

4.3.2   Other Pressure Drops

The liquid pressure drop is given by

$$\Delta p_l = \frac{\mu_l}{KA_w\rho_l h_{fg}}Q_e L_{eff} \tag{4.17}$$

Where K is the wick permeability and is given by an empirical relation

$$K = \frac{A(X^2-1)}{X^2+1} \tag{4.18}$$

$$X = 1+\frac{Bd^2\varphi^3}{(1-\varphi)^2} \tag{4.19}$$

$$A = 6\times10^{-10}m^2$$

$$B = 3.3\times10^7 m^{-2}$$

The pressure drops due to phase change at the evaporator, Δp_e, and the condenser, $\Delta p_{c,\ddot{a}}$, are very small and can be neglected .The hydrostatic pressure drop has two components, normal hydrostatic pressure drop Δp and axial

$$\Delta p_\perp = \rho_l g D_v \sin \phi \tag{4.20}$$

$$\Delta p_{\shortparallel} = \rho_l g L_t \cos \phi \tag{4.21}$$

Depending on the inclination ö of heat pipe the axial pressure drop either assists or works against the capillary pumping pressure

4.3.3 Capillary Limit

Combining Equation expression for capillary limit

$$\frac{2\sigma}{r_{eff}} = \left[\frac{\mu_l}{K A_w \rho_l h_{fg}} + \frac{(f \, \mathrm{Re}_z) \mu_v}{2 R_v^{\,4} A_v \rho_v h_{fg}} \right] Q_e L_{eff} \pm \rho_l g L_t \cos\phi + \rho_l g D_v \sin\phi \tag{4.22}$$

Let the liquid and vapor frictional coefficients be respectively defined as,

$$F_l = \frac{\mu_l}{K A_w \rho_l h_{fg}} \tag{4.23}$$

$$F_v = \frac{(f \, \mathrm{Re}_z) \mu_v}{2 R_v^{\,4} A_v \rho_v h_{fg}} \tag{4.24}$$

Therefore the capillary heat input limit is given by,

$$Q_{cop} = \frac{\dfrac{2\sigma}{r_{eff}} \pm \rho_l g L_t \cos \phi - \rho_l g D_v \sin \phi}{L_{eff} \left(F_l + F_v \right)} \tag{4.25}$$

This is the base relation for a straight cylindrical heat pipe that has inclination ö with respect to the vertical. It should be noted that since this heat pipe uses a wick, which allows circumferential communication of liquid, the normal hydrostatic pressure drop term has to be accounted for in the capillary limit When the heat pipe is in the horizontal position, ö is 90° and the axial pressure drop is eliminated, therefore the capillary limit is given by,

$$Q_{cop,horizontal} = \frac{\dfrac{2\sigma}{r_{eff}} - \rho_l g D_v}{L_{eff}(F_l + F_v)} \tag{4.26}$$

Similarly in the vertical orientation, the inclination is zero and there is no normal pressure drop term,

$$Q_{cop,vertical} = \frac{\dfrac{2\sigma}{r_{eff}} \pm \rho_l g L_t}{L_{eff}(F_l + F_v)} \tag{4.27}$$

When the heat pipe is in gravity-assisted mode of operation, the axial pressure drop term is positive in Equation otherwise when the evaporator is on the top and the heat pipe is working against the gravity, it has a negative sign.
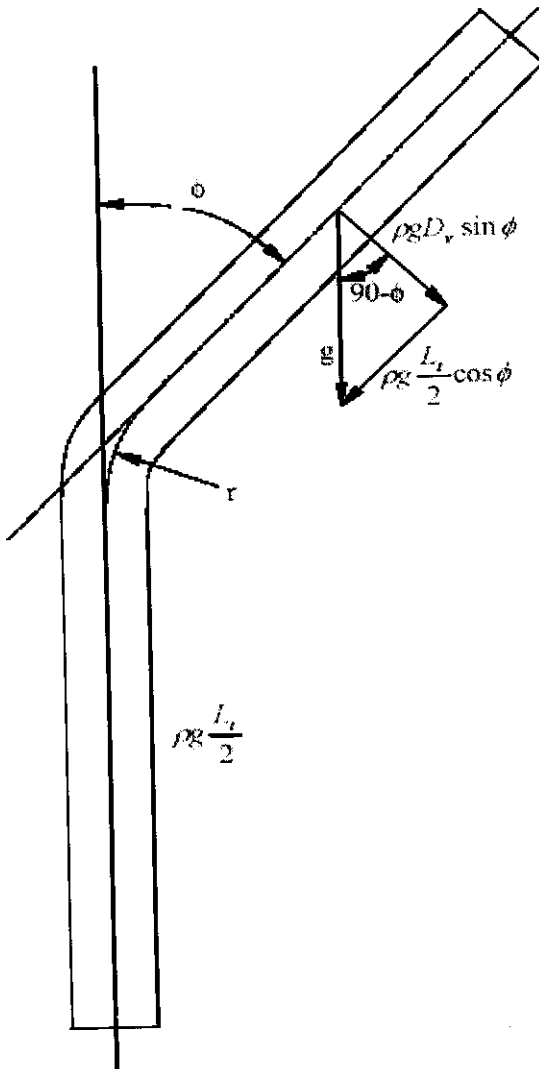
FIGURE 4.5: HYDROSTATIC PRESSURE DROPS IN A

4.3.4 OTHER LIMITS

In addition to the capillary limit, other performance limits were also calculated to check if they could be responsible for heat pipe failure. The relations required for these limits were used from available literature and are listed below,

$$Q_{sonic} = 0.474 A_v \rho_v h_{fg} \left[\frac{\gamma_v R_v T_0}{2(\gamma_v + 1)} \right]^{\frac{1}{2}} \tag{4.28}$$

$$Q_{entertainment} = A_v h_{fg} \left[\frac{\sigma \rho_v}{2 R_{h,s}} \right]^{\frac{1}{2}} \tag{4.29}$$

$$Q_{boiling} = \frac{2 \Pi L_e k_{eff} T_v}{h_{fg} \rho_v \ln\left(\frac{r_i}{r_v}\right)} \left[\frac{2\sigma}{r_a} - \Delta p_{cop, max} \right] \tag{4.30}$$

4.3.5 BEND LOSS

When a pipe is bended, there is an additional pressure drop caused primarily due to result of secondary flow and is usually represented by an equivalent length of a straight pipe The secondary flows are rotating motion, normal to the pipe axis and are superimposed on the main flow in the direction of the axis. The friction at the pipe walls and the centrifugal force combine to produce these rotations .The bend loss can be accounted for as a function of dynamic pressure of the vapor,

$$\Delta p_{bend} = K_b \frac{\rho w^2}{2}$$

$$= K_b \frac{Q_e^2}{2 \rho A_v^2 h_{fg}} \tag{4.31}$$

Most of the available data in the literature relate this loss to the relative radius of the curvature, R_v or the Dean number, De and account for the bend angle in terms of the length of the curvature. The technical paper No. 410 by the Crane

relation provided by the Crane Company is for turbulent flows in bends of 90°. Also the published work on evaluating bend losses is for losses in pipelines and their joints and fittings for turbulent flows. The work available on laminar flow is very limited and the only reported study included experimental results for a loss factor K_b as a function of the Reynolds number .The data is available for some limited radii ratios of 4.52, 6.08, 13.06 and 23.42. The data indicates that as the Reynolds number increases the friction factor for the bend decreases.

H. Ito] and Misra et al. have published results of their work on the laminar flows in curved pipes. Both of them have produced similar relations for the relative friction factor of a curved pipe in terms of the Dean number.

The relation by Ito is

$$\frac{f_b}{f_r} = .63416 De^{\frac{1}{2}} \left[\left(1 + \frac{6.11541 \times 10^{\frac{1}{2}}}{De} \right)^{\frac{1}{2}} - \frac{2.472935}{\sqrt{De}} \right]^{-3} \qquad (4.32)$$

For laminar flow through a bend of angle ö, the bend loss is a sum of the pressure drops due to bend and frictional pressure drops in a straight pipe of an equivalent length. This results in a relation between friction factor f_b for bends and friction factor f_s for the straight sections.

$$\Delta p_b = K_b \frac{w^2}{2} + \Delta p_s$$

$$\frac{f_b L_b w^2}{4 R_V} = K_b \frac{w^2}{2} + \frac{f_s L_b w^2}{4 R_v} \qquad (4.33)$$

Where, K_b is bend loss coefficient and L_b is length of bend.

$$\frac{f_b r \phi}{2 R_V} = K_b + \frac{f_s r \phi}{2 R_v} \qquad (4.34)$$

Bend Loss Coefficient for Vapor Flow

$$\left[\qquad \frac{1}{2} \left[\quad 1.729 \right]^{\frac{1}{2}} \quad 1.315 \right]^{-3}$$

The above relation was directly used in the calculations for the capillary limits reported in the following section.

4.3.6 CAPILLARY LIMIT FOR BENDED HEAT PIPE

It was proposed in the last two sections that the effect of the bending angle could be accounted for by representing the bending losses as a function of the axial velocity. Due to various possible orientations of a bended heat pipe, expressions for the capillary limit in various orientations are given below

Heat pipe oriented horizontally

$$Q_{cop,horizontal} = \frac{\dfrac{2\sigma}{r_{eff}} - \rho_l g D_v - \left(K_b \dfrac{Q_e^2}{2\rho A_v^2 h_{fg}^2} \right)}{L_{eff}\left(F_l + F_v\right)} \tag{4.36}$$

Heat pipe oriented vertical gravity assisted orientation

$$Q_{cop,vertical} = \frac{\dfrac{2\sigma}{r_{eff}} + \rho_l g \dfrac{L_t}{2}\left(1+\cos\phi\right) - \rho_l g D_v \sin\phi - \left(K_b \dfrac{Q_e^2}{2\rho A_v^2 h_{fg}^2} \right)}{L_{eff}\left(F_l + F_v\right)} \tag{4.37}$$

Heat pipe in a vertical adverse gravity orientation

$$Q_{cop,vertical,adverse} = \frac{\dfrac{2\sigma}{r_{eff}} + \rho_l g \dfrac{L_t}{2}\left(1+\cos\phi\right) - \rho_l g D_v \sin\phi - \left(K_b \dfrac{Q_e^2}{2\rho A_v^2 h_{fg}^2} \right)}{L_{eff}\left(F_l + F_v\right)}$$

Chapter 5

Computational Fluid
Dynamics

5.1 INTRODUCTION

Fluid flow is governed by the conservation of three fundamental quantities namely mass, momentum and energy. The description of these conservation laws in mathematical form yields non-linear partial differential equation, which is famously known as the Navier-stroke equation. Although these Navier-stroke equations have been known since the 1800s, they have been too difficult to solve for arbitrary flows until the development of the modern computer. The science involved in solving these equations numerically on the computer is known as computational fluid dynamics (CFD)

In order to solve the Navier-Stokes equations, the flow domain for the specific problem is first discretised. Domain discretisation, using mesh or grid generating techniques, involves breaking up the selected control volume into smaller volumes and solving the Navier-Stokes equations over each volume. For simple geometries such as rectangular shapes, discretisation is simple but gets more difficult as the geometry becomes more complex. Also, to accurately capture flow phenomena such as turbulence, fine grids are required at the region of interest leading to an increased number of mesh elements. This results in a large system of non-linear equations requiring large computing memory. However, with the ever-increased computing capability available today, a lot of complex flow problems can now be solved.

Commercial CFD codes such as FLUENT, PHOENIX, CFX, CFD++ and Star-CD have also developed to a point that the user need not be an expert on CFD in order to successfully put it to use. The end-user must however have a good knowledge of fluid dynamics for a successful simulation with credible results to be obtained. Therefore, used correctly, CFD codes can reduce time and cost of experiments in product development or process improvement.

The rest of the chapter discusses the various areas of CFD in the following order:
- Governing equations
- Grid generation techniques

• Solution algorithms and convergence criteria
• Basic background on the CFD solver used (FLUENT)

5.2   GOVERNING EQUATIONS

The governing equations of fluid behavior are given in equations. These equations are given for compressible flow, but can be easily simplified for incompressible flow. In the Eulerian system, the particle derivative is described as follows

$$\frac{D}{Dt} = \frac{\partial}{\partial t} + \left(\overline{V} . \nabla \right)$$
(5.1)

Where:

$$\left(\overline{V} . \nabla \right) = d\overline{V} = \frac{\partial u}{\partial x} + \frac{\partial V}{\partial y} + \frac{\partial w}{\partial Z}$$
(5.2)

This particle derivative will be used in the sections to follow to present the Navier-Stokes equations in conservative form.

5.2.1 Conservation of Mass

The equation for conservation of mass in conservative form is given as:

$$\frac{\partial \rho}{\partial t} + \nabla . \left(\rho \overline{V} \right)$$
(5.3)

Where ρ is the density and $\overline{V}$ is the vector velocity of the fluid.

5.2.2 conservation of Momentum

The equations for conservation of momentum in the three Cartesian directions can be written as a single vector equation using indicial notation:

$$\frac{D\rho\overline{V}}{Dt} = \rho\overline{g} - \Delta p + \frac{\partial}{\partial x_j}\left[\mu\left(\frac{\partial v}{\partial x_j} + \frac{\partial v_j}{\partial x_i} \right) + \delta_{ij} \lambda d\overline{V} \right]$$
(5.4)

5.2.3 The Energy Equation

The energy equation, which in essence is the first law of thermodynamics, is given in its most economic form as follows:

$$\rho \frac{D}{Dt}\left[e + \frac{p}{\rho} \right] - \frac{Dp}{Dt} + d\left(K\nabla T \right) + \tau_{ij}\frac{\partial u_i}{\partial x_j} \tag{5.5}$$

Where the viscous stresses are given by the stress tensor:

$$\tau_{ij} = \mu\left(\frac{\partial u_i}{\partial x_j} + \frac{\partial u_j}{\partial x_i} \right) \tag{5.6}$$

5.3 TWO-EQUATION MODEL: *K- α MODEL*

Engineering flow problems encountered in CFD are often turbulent, thus requiring more effort to solve. Turbulent flows are described by disorderly (or 'chaotic') motion of fluid particles in space and time. The degree of unsteadiness of the flow is often subject to the complexity of the geometry. Flow fluctuations bring into contact particles of differing momentum resulting in velocity reductions due to viscous effects; subsequently the kinetic energy is reduced. This process is said to be dissipative.

Turbulence also increases mixing of particles thereby differing concentrations of conserved quantities are mixed. This process is called turbulent diffusion. Turbulence, depending on the application, can have desirable effects, for example; chemical mixing and increased wall heat transfer coefficients for better heat transfer rates than in laminar flow. In other applications, turbulence is required though it may lead to losses. Such an application is flow into the combustion chamber where mixing of fuel and air is desired, but because of turbulence, flow velocity is reduced.

Most compressible viscous flow is turbulent, thereby increasing the

the phenomenon. Turbulence modeling is based on the principle that unsteady and irregular high-Reynolds-number flow averaged over time is steady and predictable. This principle leads to a set of non-linear differential equations known as the Reynolds-Averaged Navier-Stokes (RANS) equations. For high-Reynolds number compressible flow; viscous and turbulent effects are only significant near the walls, as a result the turbulent models need only be applied to a small section of the computational domain.

Turbulent models comprise, in order of complexity, among others the zero-equation model, one-equation model (turbulent kinetic energy), two-equation model (e.g., k-ε model), Reynolds stress model (RSM) and large eddy simulation (LES). Direct numerical simulation is the highest level of turbulence simulation, as it requires the exact solution of the full Navier-Stokes equations without averaging or approximation. Since the cost of simulation is directly proportional to Re3 and also due to computer capability limitations, DNS is currently only possible for flows of low Reynolds (Re) numbers and simple geometrical domains.

As there are many suggested turbulence models today, only the best-suited model for each application need be used and for this study the k-ε model proved sufficient for the simulations. The k-ε model is a two-equation model coupling the turbulent kinetic energy equation with the equation for modeling the rate of change of dissipation (ε). The resulting two models are given below for fully elliptic high-Reynolds-number flow.

$$\frac{D\varepsilon}{Dt} \approx \frac{\partial}{\partial x_j}\left[\frac{v_i}{\sigma_\varepsilon}\cdot\frac{\partial \varepsilon}{\partial x_j}\right] + C_1 V_1 \cdot \frac{\varepsilon}{k}\cdot\frac{\partial \overline{u_i}}{\partial x_j}\left[\frac{\partial \overline{u_i}}{\partial x_j} + \frac{\partial \overline{u_j}}{\partial x_i}\right] - \frac{C_2 \varepsilon^2}{k} \qquad (5.7)$$

$$\frac{Dk}{Dt} = \frac{\partial}{\partial x_j}\left[\frac{v_i}{\sigma_k}\cdot\frac{\partial k}{\partial x_j}\right] + v_i \cdot \frac{\partial \overline{u_i}}{\partial x_j}\left[\frac{\partial \overline{u_i}}{\partial x_j} + \frac{\partial \overline{u_j}}{\partial x_i}\right] - \varepsilon \qquad (5.8)$$

Where $\sigma k = vt/vK$ and $\sigma\varepsilon = vt/v\varepsilon$ are effective "Prandtl numbers" relating eddy diffusion of k and ε to the momentum eddy viscosity. The eddy viscosity is modeled as follows:

$$v_t = \frac{\mu_1}{\rho}$$

(5.9)

Recommended values for attached boundary layer calculations of the five empirical constants are given below:

TABLE5.1: RECOMMENDED VALUE FOR EMPIRICAL CONSTANT

C_μ	C_1	C_2	σ_k	σ_ξ
0.09	1.44	1.92	1.0	1.3

The values are however, not universal and need to be modified for different problems such as jet, wakes, and recirculating flows. The combination of the equations, empirical constants in Table, continuity and the momentum relations yields a system of equations that are simultaneously solved with turbulent closure to as the k-ε model. Near the wall, the k-ε model is not valid and thus a curve-fit incorporating the laminar sub layer (law of the wall) and the logarithmic layer (log law), known as a wall function, is used. The k-ε computations begin at a certain distance y away from the wall. The log-law belongs to a class of models known as wall functions.

5.4   NEAR-WALL TREATMENT

Due to the viscous and sub-layer damping effects in the turbulent boundary layer, the Reynolds number is significantly lower in this region. At high Reynolds number flows, the k-ε model requires a very fine grid at the turbulent boundary layer to solve for the flow properties in this region. This is due to the fact that the boundary layer is very thin at high Reynolds numbers. Due to the computational effort a fine grid requires, wall functions are used near the wall.

The relations given in are for the velocity profile in the turbulent boundary layer.

$$u^+ = \frac{\overline{v_t}}{u_\tau} = \begin{cases} n^+ \quad - - - - - - - - n^+ \le 5 \\ \dfrac{1}{k} \ln\left(n^+\right) + B \ - - - \ n^+ > 30 \end{cases}$$

Where $\overline{v_t}$ the mean velocity is parallel to the wall and u_τ is the shear velocity given

by: $u_\tau = \sqrt{\dfrac{\tau_w}{\rho}}$ \hfill (5.10)

Where τ_w is the shear stress at the wall, κ is the von Karman constant ($\kappa = 0.41$) and B is an empirical constant related to the viscous sub-layer ($B = 5$).

In equation, the dimensionless distance from the wall given by

$$n^+ = \frac{\rho u_\tau n}{\mu} \hfill (5.11)$$

In most literature n^+ is also referred to as y^+. The log-law is valid for: $30 < y^+ < 60$.
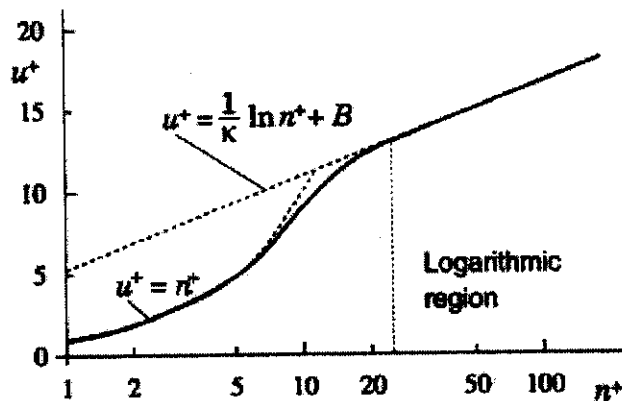

FIG.5.1: VELOCITY PROFILE AS FUNCTION OF DISTANCE NORMAL TO THE WALL

Figure5.1 illustrates the velocity profile as a function of distance normal to the wall. Dashed lines are from corresponding equations whereas the solid line constitutes averaged experimental data.

5.5 GRID GENERATIONS AND GAMBIT

The grid generation process or meshing involves dividing the flow domain into smaller control volumes over which the discretised Navier-Stokes equations are solved. Grid (mesh) types can be classified into two categories namely; structured and unstructured grids. The mentioned types of grids find use in different applications and are used in the meshing process in this study.

Structured grids consist of grid lines with a characteristic of not crossing or overlapping. The position of any grid point is uniquely identified by a set of two (2-D) or three (3-D) dimensional indices, e.g., (i, j, k). Unstructured grids make no assumption about any structure in the grid definition and usually consist of triangular (tetrahedral (ted) in 3D) elements.

A numerically generated structured grid or mesh is understood here to be the organized set of points formed by the intersections of the lines of a boundary conforming to a curvilinear coordinate system. The prime feature of such a system is that some coordinate line (surface in 3D) is coincident with each segment of the boundary of the physical region.

The use of coordinate line intersections to define the grid points provides an organizational structure that allows all computations to be done on a fixed square grid when partial differential equations of interest have been transformed so that the curvilinear coordinates replace the Cartesian coordinates as the independent variables. This grid frees the computational simulation from restriction to certain boundary shapes and allows general flow solvers to be written in which the boundary shape is specified simply by input.

Grid generation for the purposes of this research takes place in FLUENT's pre-processor, GAMBIT. GAMBIT is a versatile pre-processor that can support a large variety of commercially available computer-aided design (CAD) platforms. Raw geometry can be imported from these CAD packages into GAMBIT where it is operated on (i.e., the necessary simplification for CFD purposes are made), in

Various meshing schemes are available in GAMBIT and are used where suitable in the grid generation process. Most of these schemes are unique to GAMBIT and are not necessarily documented, as they may be modifications of existing meshing schemes.

GAMBIT allows the user to specify any volume to be meshed, although the shape and topological characteristics of the volume determine which mesh schemes can be used.

Different meshing schemes such as Hex, Hex/wedge and Tet Hybrid, can be specified on volumes to be meshed. The Hex mesh is composed of hexahedral elements only constituting a fully structured mesh. The Hex/wedge mesh comprises mainly of hexahedral elements with wedge elements where necessary. However, Hex and Hex/wedge elements do not apply to any shape volume, as opposed to Tet Hybrid meshes. The versatility of the Tet Hybrid element makes it appreciable for use where the volume is complex and none of the other meshes can be applied. Solution inaccuracies associated with the Tet Hybrid element type are, however, more significant than for any of the other element types. Each element type is associated with a volume-meshing scheme and only those schemes used in this study will be discussed.

Cooper meshing scheme

When this scheme is enforced on a volume, GAMBIT treats the volume like a cylinder with end-caps. In the actual volume, the faces at these locations are representative of the end-caps and are called source faces as in Figure. They are so-called because Figure 5.2 illustrates their face meshes are projected through the volume after certain mesh operations have been performed by GAMBIT as.

(a) Original volume   (b) Logical cylinder
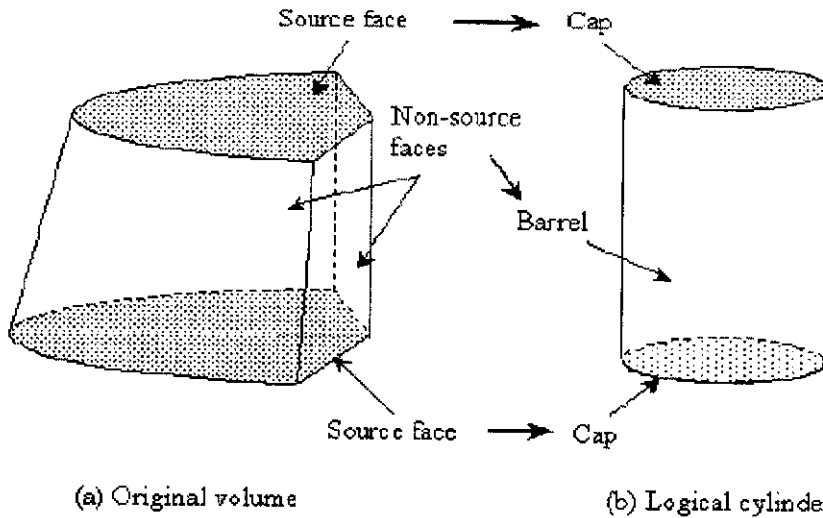
**FIG.5.2: COOPER MESHING SCHEME VOLUME
TREATMENT**

The Cooper scheme involves, in order of occurrence, the following steps:

1. Meshing the non-source faces

2. Imprinting the source faces on one another

3. Meshing the source faces

4. Projecting the source faces' node patterns through the volume to
produce a   Volume mesh

The steps described can be illustrated by the example in Figure 5.3, which shows
the union of a prism, cylinder and a rectangle.

FIG.5.3: UNION OF CUBE, A CYLINDER, AND A

The various Cooper mesh scheme steps are clearly illustrated in Figure 5.4.
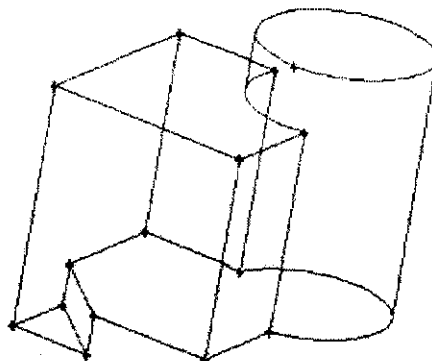

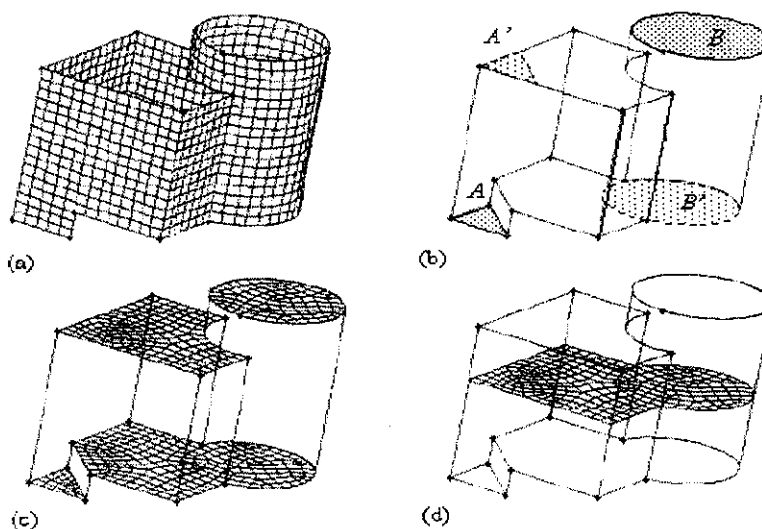(a)　　　　　　　　(b)

(c)　　　　　　　　(d)

FIG.5.4: COOPER MESHING SCHEME

5.6　BOUNDARY CONDITIONS

Equations presented in the preceding section remain the same regardless of the flow field, i.e., external flow, internal flow, two-phase flow (with some modifications), etc. In mathematics, any solution to a set of partial differential equations (PDE's) requires a set of boundary conditions for closure and the solution of the governing equations is no exception.

CFD simulations largely depend on the boundary conditions specified; hence correct boundary specification improves convergence to a correct solution. Incorrect boundary and initial conditions, however, can give convergence although not to a correct solution. There is a wide variety of boundary types available in FLUENT, but only those used in this study will be given.

1) Flow inlet and exit boundaries

Pressure inlet: Used to define the total pressure and other scalar quantities at flow inlets.

boundary condition instead of an outflow condition often results in a better rate of convergence when backflow occurs during iteration. Note that when backflow occurs, this boundary acts like a pressure inlet boundary.

2) Wall and symmetry:

Wall: Used to define a solid-fluid interface where viscous flow is considered, thus applying a no-slip condition. The boundary condition on a surface assumes no relative velocity between the surface and the gas immediately at the surface.

Symmetry: Used to define surfaces at which normal velocity and normal gradients of all other variables are zero. This boundary type is essential where the geometry is symmetrical in nature.

5.7   SOLUTION ALGORITHMS

The governing equations of fluid flow are particularly difficult to solve because of their non-linear nature. Much work has been done in numerical methods to solve for these types of equations. Some proven and popular methods worthy of note are SIMPLE, and PISO. These methods are appreciated because of their robustness when applied to a variety of problems. In this study, steady-state and transient flows are solved using the SIMPLE and PISO algorithms respectively.

The acronym, SIMPLE, stands for Semi-Implicit Method of Pressure-Linked Equations, and describes the iterative procedure by which a solution to discretised equations is obtained. This method is well suited to steady-state solution computation. The iterative procedure is the pseudo-transient treatment of the unsteady governing equations in a discrete form to obtain a steady-state solution. Patankar and Spalding introduced SIMPLE. The SIMPLE algorithm has a limitation in that new velocities and corresponding fluxes do not satisfy the momentum balance after the pressure-correction equation is solved. As a result,

improves the efficiency of this calculation by performing two additional corrections namely, neighbour and skewness correction.

PISO, which stands for Pressure-Implicit with Splitting of Operators, is a pressure-velocity coupling scheme that is part of the SIMPLE family of algorithms. This scheme is based on the higher degree of the approximate relation between the corrections for pressure and velocity. In highly distorted meshes, the approximate relationship between the correction of mass flux at the cell face and the difference of the pressure corrections at the adjacent cells is very rough. An iterative process is required to solve for the pressure-correction gradient components along cell faces since they are not known beforehand leading to the introduction of a process named skewness correction . Here, the pressure-correction gradient is recalculated and used to update the mass flux corrections after the initial solution of the pressure-correction equation is obtained. This process significantly reduces convergence difficulties associated with highly distorted meshes and allows FLUENT to obtain solution on a highly skewed mesh in approximately the same number of iterations as required for a more orthogonal mesh. The PISO algorithm is used in this study for calculation of the unsteady gas behaviour due to its efficient nature and suitability for transient computations as recommended in FLUENT.

5.8 CONVERGENCE

Convergence of a flow or heat problem can be judged by observing the normalized residuals. Residuals are numerical imbalances from the solved governing equations resulting from an incomplete solution during the iterative process. The solution process can be terminated when the normalized residuals fall below a specified value, which is generally 10^{-3}. However, in some cases even with the convergence criteria (as far as normalized residuals are concerned) satisfied, the solution may not necessarily be a correct one. To avoid such instances, quantities such as mass flow rate, static pressure and heat flux can be monitored at a location in the flow domain that is deemed to be important. The monitored quantity is observed until the change from iteration to iteration is

5.9   BACKGROUND ON THE CFD SOLVER USED(FLUENT)

FLUENT is a finite volume (FV) solver that can handle a wide variety of flow problems such as external flow, internal flow, and two-phase flow. All modes of heat transfer can also be solved by the CFD code. This code is used for all CFD analyses throughout this study.

Modern CFD packages are user-friendly with improved user and code interfacing. Thus understanding the underlying principles of flow is important in order to put the code to good use. FLUENT has a facility for coding to make repetitive simulations, as in an optimization loop, more efficient and hence save time. This facility makes use of a journal file, which is a file containing a list of text commands that set-up a CFD model and runs the simulation. Post processing can also be performed with the use of these journal files.

The code developers validate and verify chosen simulated flow cases (mostly from industrial users) against experimental data, consequently ensuring a validated code for users. Thus, the code is very suitable for a wide-variety of industrial problems including the one that is the subject of this study, as will be seen in the chapters that follow.

As discussed in this section, the solution to the Navier-Stokes equations cannot be determined analytically; hence it is solved at discrete points in the flow domain by an iterative process. The various important aspects of grid generation process were also discussed as well as boundary condition specification. Solution algorithms used in solving the governing equations were briefly discussed as well as the solution convergence. The code, FLUENT, used in the study was also discussed where its journal file function's efficiency was highlighted in being the main point making FLUENT suitable for optimization problems.

Chapter 6

Results and Discussions

6.1.BENDING CONFIGURATIONS FOR HEAT PIPE

Heat pipe were tested for studying the concept of bendable heat pipes. The heat pipes tested consisted of a wick made from the sintered copper felt with water as the working fluid. The first set of tests were carried out on Heat pipe and included testing in horizontal, vertical gravity assisted and bended in the vertical gravity assist orientation for the angles of 15°, 30°, 45°, 60° and 90°
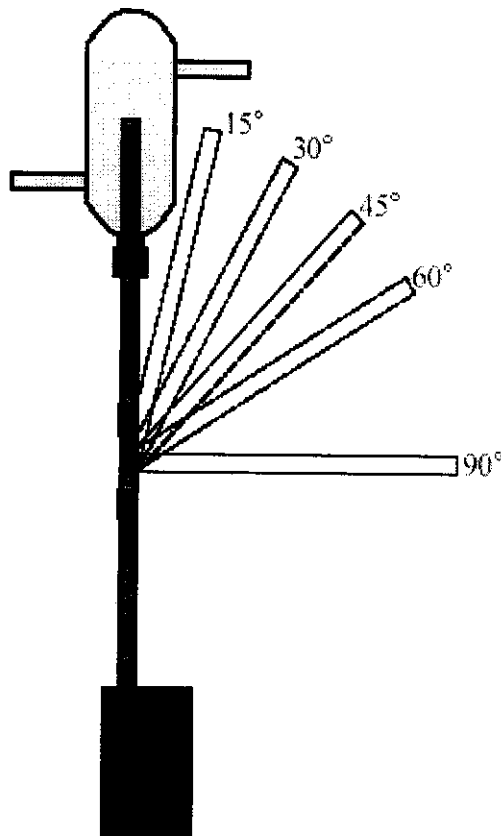

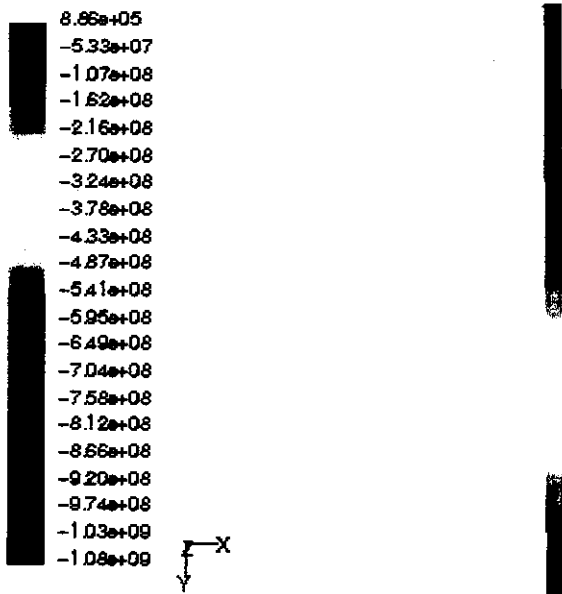**FIG. 6.1: SCHEMATIC OF BENDING CONFIGURATIONS FOR HEAT PIPE**

6.2. SPECIFICATIONS OF HEAT PIPE

- Container outer diameter (D) – 8.00 mm
- Working length (L) – 260.2 mm
- Evaporator length (L_e) – 30.1 mm
- Condenser length (L_c) – 30.1 mm
- Adiabatic section length (L_a) – 200 mm
- Sintered metal felt wick thickness – 0.3175 mm
- Porosity (ö) – 87%
- Length of metal felt strands – 10 mm
- Diameter of metal felt strands – 3.5 x 10^{-2} mm
- Charge – 1.3g
- Permeability – 442.76 μm^2

6.3. HEAT PIPE TEST RESULTS

- Straight
- 15° bended vertical
- 30° bended vertical
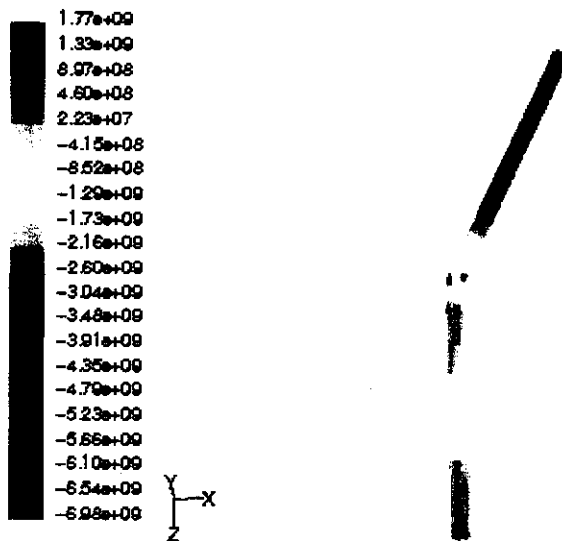- 45° bended vertical
- 60° bended vertical
- 90° bended vertical

Vertical refers to gravity-assisted operation.

8.86e+05
−5.33e+07
−1.07e+08
−1.62e+08
−2.16e+08
−2.70e+08
−3.24e+08
−3.78e+08
−4.33e+08
−4.87e+08
−5.41e+08
−5.95e+08
−6.49e+08
−7.04e+08
−7.58e+08
−8.12e+08
−8.66e+08
−9.20e+08
−9.74e+08
−1.03e+09
−1.08e+09

Contours of Static Pressure (pascal)   Apr 17, 2006
                                              FLUENT 6.1 (3d, segregated, ske)

FIG.6.2: TEST RESULTS FOR IN STRAIGHT HEAT PIPE

1.77e+09
1.33e+09
8.97e+08
4.60e+08
2.23e+07
−4.15e+08
−8.52e+08
−1.29e+09
−1.73e+09
−2.16e+09
−2.60e+09
−3.04e+09
−3.48e+09
−3.91e+09
−4.35e+09
−4.79e+09
−5.23e+09
−5.66e+09
−6.10e+09
−6.54e+09
−6.98e+09

Contours of Static Pressure (pascal)   Apr 17, 2006
                                              FLUENT 6.1 (3d, segregated, ske)

FIG.6.4: TEST RESULTS FOR IN 30° BENDED HEAT PIPE

Contours of Static Pressure (pascal)   Apr 17, 2006
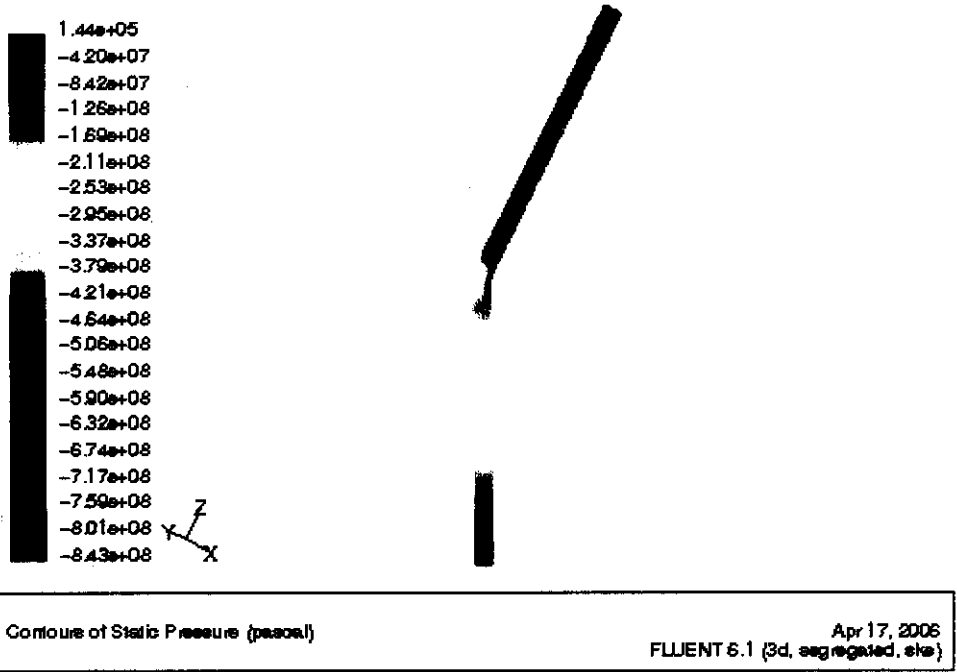   FLUENT 6.1 (3d, segregated, ske)

FIG.6.6: TEST RESULTS FOR IN 60° BENDED HEAT PIPE

Contours of Static Pressure (pascal)   Apr 17, 2006
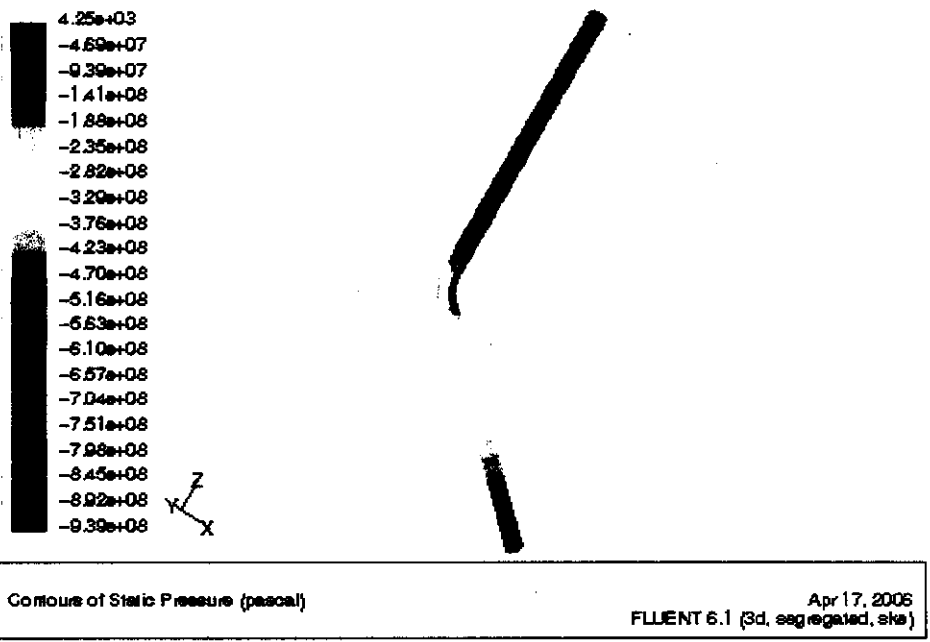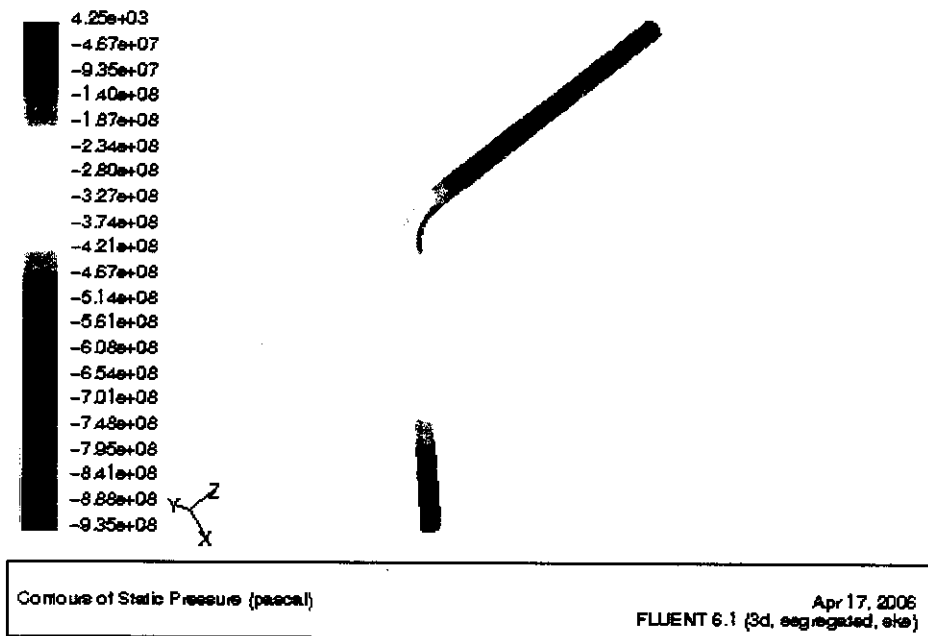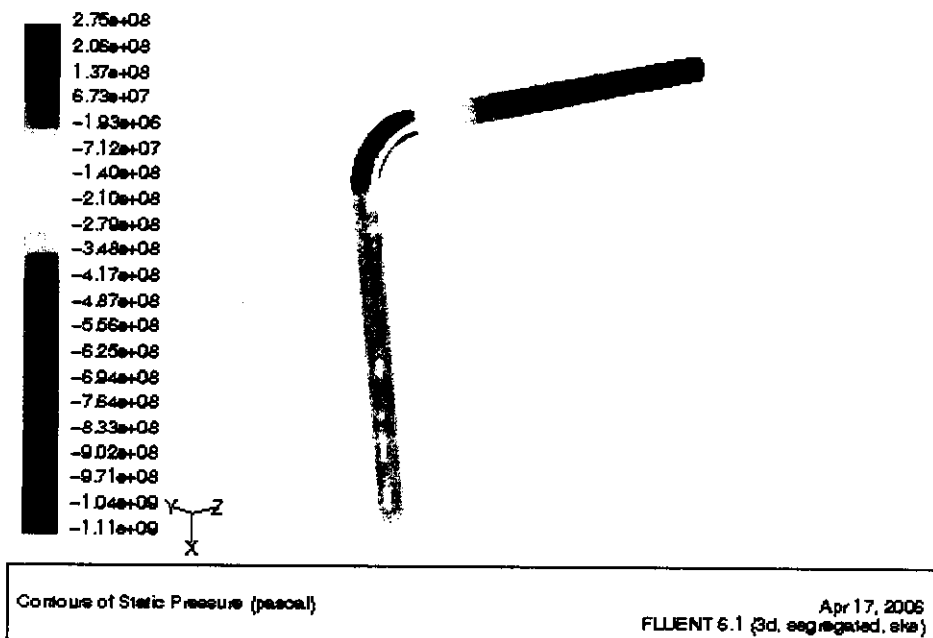   FLUENT 6.1 (3d, segregated, ske)

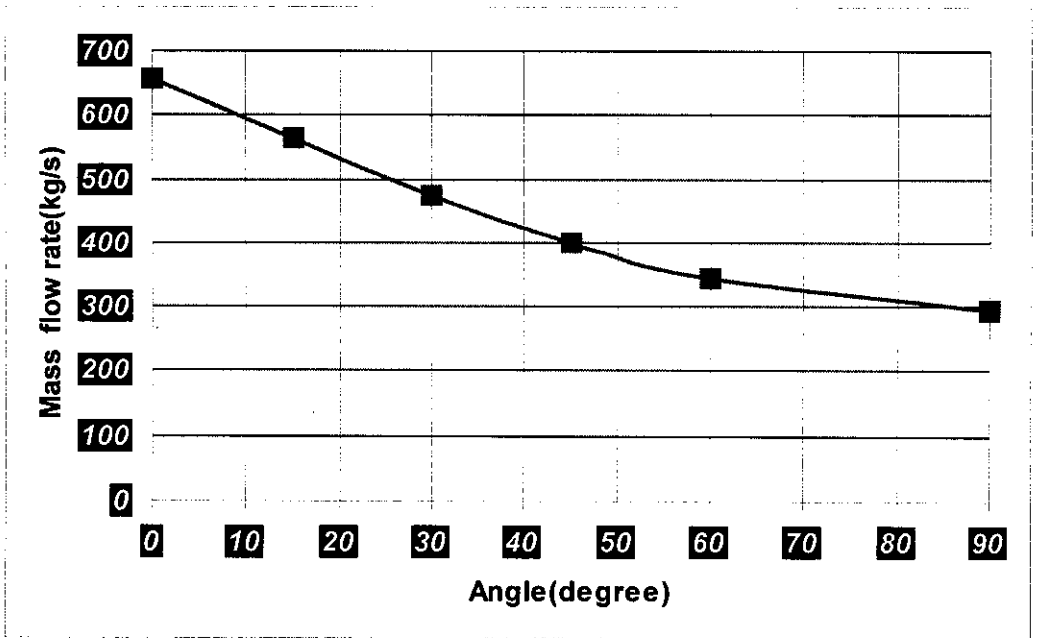**FIG.6.7: TEST RESULTS FOR IN 90° BENDED HEAT PIPE**
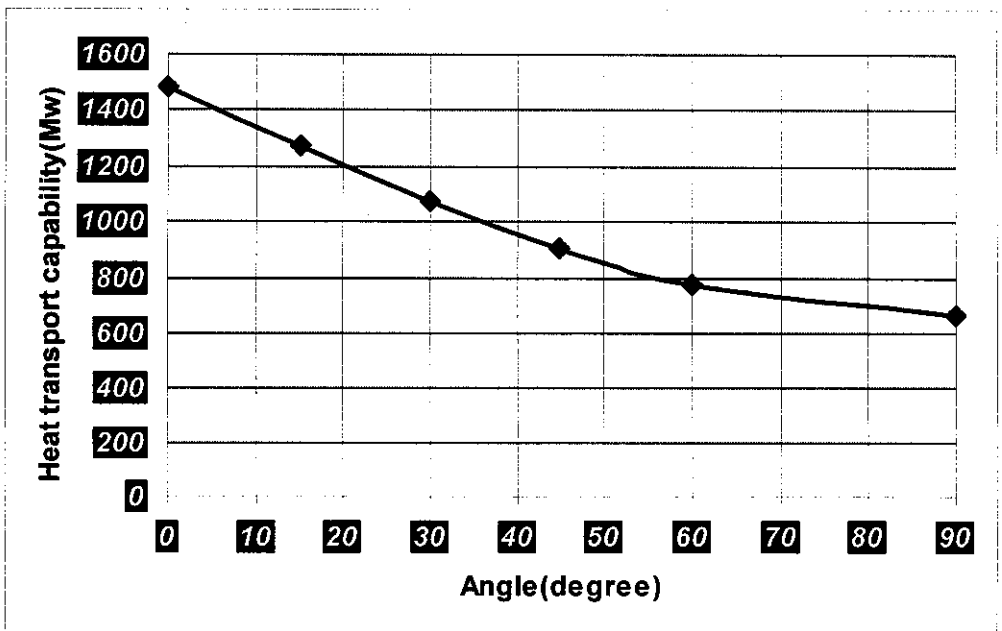
FIG. 6.8:ANGLE VS MASS FLOW RATE

FIG.6.9: ANGLE VS HEAT CARRYING CAPABILITY

6.4.DISCUSSIONS

It has inferred from the data obtained that as the pipe bend angle was increased, the mass flow rate of the fluid water and its heat carrying capacity decreased

When the heat pipe was in horizontal orientation the axial gravitational pressure drop was absent, capillary pumping pressure was the only driving factor. Therefore, all tests in horizontal orientation show a trend towards the capillary limit curve. Therefore, the possibility of encountering capillary limit in horizontal orientation was high.

Since the boiling limit is a radial flux limitation, it was found that the heat pipe was limited by boiling phenomenon in situations where the capillary limit was high and the operating temperatures and input heat flux were high enough to initiate nucleate boiling. Due to limitation of software resources, this aspect could not be investigated.

During calculations of energy losses in the bended section of the heat pipe, it was found that it was very minimal and practically incapable in affecting the capillary limit. This can be explained by considering the Reynolds numbers for the vapor flow. The vapor flow was laminar for all the calculations and Reynolds number was in the range of 10-900. The fluid having low density and the high viscosity minimized the expected losses due to centrifugal forces at the bend and hence the frictional pressure drop was negligible.

Chapter 7

Conclusion

The aim of this analysis was to demonstrate the feasibility of various bends in heat pipe. A detailed literature review showed that flexible heat pipes have attracted a lot of attention over the years. But all of the work published previously was geared towards making pipes, which were either flexible or pre-bended during fabrication. It was found that no attempt was made to explore the possibility of stock heat pipes, which can be bended or flexed in different shapes as required by the target application.

The ongoing work on heat pipes made using sintered copper matting as the wicking medium was extended to explore this possibility. The results for various bends in heat pipe are encouraging as the heat pipe was found to work well in all orientations and up to a bend of 90°. The effect of pressure loss due to bending was found to be negligible and three to four orders of magnitude smaller than the capillary pumping pressure. This shows that the increase in the temperature drop due to bending is because of the obstruction in the flow of liquid returning to the evaporator from the condenser. The investigation of wick separation due to bending showed a noticeable separation of the wick from the container walls. The vapor flow area was also reduced that directly reduced the heat carrying capacity.

7.1. FUTURE WORK

The possibility of multiple bends needs to be explored for this concept to be Feasible in practice. The current heat pipes were found to be capable of working after multiple bends although no systematic testing was carried out. The possibility of the heat pipe working beyond 90° could also be explored.

Similarly, the aspect of different combinations of working fluids and wicking mediums could also be explored. This will allow testing of various bends in heat pipe at different operating temperature ranges. The effect of relative radius of curvature on the heat pipe performance needs further investigation. This aspect is slightly complex as once bent, the same heat pipe might be damaged if the bending radius is changed later. There is a possibility that the diameter of the heat pipe will play some role in the number of bends that can be introduced in the heat pipe. This could be investigated by testing a batch of heat pipes of different sizes.

References

1) Basiulis and. Hummel, T. A "The application of heat pipe techniques to electronic component cooling", *ASME Winter Annual Meeting*, New York, 1972.

2) Bliss Jr., F. E. Clark Jr. E. G. and Stein, B. "Construction and test of a flexible heat pipe", *ASME Conference Paper*, 1970.

3) Dunn, P. D. and Reay, D. A. Heat pipes, 4th Ed, U.S.A., Pergamon, 1994.

4) Edelstein, F. "Deployable heat pipe radiator [Final Report]", *NASA Report*, 1975.

5) Ernst, D. M. and Eastman, G. Y. "High temperature heat pipe technology at Thermacore – an overview", *AIAA 20th Thermophysics Conference*, Williamsburg, 1985.

6) Faghri, Heat pipe science and technology. Washington, D.C., Taylor & Francis, 1995

7) Gernert, N. J. and Brown, J. "Development of a flexible loop heat pipe cold plate", *SAE Aerospace Atlantic Conference*, Dayton, 1995

8) Groll, M., Muenzel, W. D., Supper, W. and Savage, C. J. "Development of an axial groove aluminum-ammonia liquid trap heat pipe thermal diode", 3rd *International Heat Pipe Conference*, Palo Alto, 1978.

9) Gus'kov, A. S. Gortyshov, Y. F. and Poskonin, Y. A. "Calculation of the thermophysical characteristics of an arterial flexible heat pipe", *Izvestiya Vysshikh Uchebnykh Zavedenij. Aviatsionnaya Tekhnika*, no. 4, pp. 38-43. 1993

10) Hwangbo, H. A. N and Joost, T. E. "A flexible variable conductance heat pipe design for temperature control of spacecraft equipment", *AIAA Thermophysics, Plasma dynamics and Lasers Conference*, San Antonio, 1988.

11) Ivanovskii, M.N, Sorokin, M.N, and Yagodakin, I.V. The physical principles of heat pipes, 1982

12) Koch, H., Kreeb, H. and. Perdu, M "Modular axial grooved heat pipes (for spacecraft radiators)", *European Space Agency Report*, 1976.

13) Mathieu, J. P., Moschetti, B. and Savage, C. J. "Development of a high performance variable conductance heat pipe", *AIAA 15th Thermophysics Conference*, Snowmass, 1980

14) Meier, K. L., Martinez, H. E. and Runyan, J. E. "Development of space reactor core heat pipes", *Intersociety Energy Conversion Engineering Conference*, Atlanta, 1981.

15) Muenzel, W. D. "Life tests of the telecommunications satellite heat pipes [Final report]", *European Space Agency report*, 1977.

16) Muenzel, W. D., Savage, C. J., Accensi, A. and Aalders, B. G. M. "Performance evaluation of the ESRO heat pipes included in the International Heat Pipe Experiment (IHPE) (using ammonia and acetone

17) Peeples, M. E. and Calhoun, L. D. "Fabrication and comparative performance of three variable conductance heat pipe concepts", *ASME Paper*, 1977.

18) Peterson, G. P. "Analytical development and computer modeling of a bellows-type heat pipe for the cooling of electronic components", *Heat Transfer Engineering*, vol. 9, no.3, pp. 101-109, 1988

19) Peterson, G. P. An Introduction to Heat Pipes – Modeling, Testing and Applications, John Wiley & Sons, Inc., 1994

20) Saaski, E. W. and Wright, J. P. "A flexible cryogenic heat pipe", *AIAA 10th Thermophysics Conference*, Denver, 1975.

21) Shaoning Lu and His-Shang Li, "Oscillatory mode with extremely high heat transfer rate in a flexible heat pipe", InterPACK *'99: Pacific RIM/ASME International Intersociety Electronics Photonic Packaging Conference 'Advances in Electronic Packaging 1999'*, Maui, 1999.

22) Shaubach, R. M and Gernert, N. J. "High performance flexible heatpipes", *AIAA 20th Thermophysics Conference*, Williamsburg, 1985.

23) Tohru Kishimoto, "Flexible-heat-pipe cooling for high-power devices", *The International Journal of Microcircuits and Electronic Packaging*, vol. 17, no. 2, pp. 98-107, 1994.

24) Wright, J. P., Brennan, P. J. and McCreight, C. R. "Development and test of two flexible cryogenic heat pipes (for spacecraft instrument cooling)", *AIAA 11th Thermophysics Conference*, San Diego, 1976.

25) Zelenov, A. Zuev, V. G. and Poskonin, U. A. "Flexible heat pipes, construction special features and test results", *ESA International Conference on Spacecraft Structures, Materials and Mechanical Testing*, pp. 1381-1384, Noordwijk, 1996.